Theses and Dissertations

5-2018

State Dependent Function and Dynamics in Cerebral Cortical Networks

Leila Fakhraei
University of Arkansas, Fayetteville

State Dependent Function and Dynamics in Cerebral Cortical Networks

A dissertation submitted in partial fulfillment
of the requirements for the degree of
Doctor of Philosophy in Physics

by

Leila Fakhraei
University of Shiraz
Bachelor of Science in Physics, 2007
University of Kerman
Master of Science in Physics, 2010
University of Arkansas
Master of Science in Physics, 2015

May 2018
University of Arkansas

This dissertation is approved for recommendation to the Graduate Council.

_____
Dr. Woodrow Shew
Dissertation Director

_____
Dr. Jiali Li
Committee Member

_____
Dr. Nathan Parks
Committee Member

_____
Dr. Pradeep Kumar
Committee Member

Abstract

Cerebral cortex exhibits vigorous ongoing, internal neural activity even with no sensory input is present or the animal is minimally engaged in a task or behavior. This internal ongoing activity is not static; the 'cortical state' varies ranging from synchronous and highly correlated activity to asynchronous and weakly correlated neural activity. The main goal of the work presented here is to understand how changes in cortical states effect several aspects of cortical function and dynamics.

To meet this goal, we did three separate projects. First, we compared the predictability of neuronal network dynamics across cortical states in somatosensory cortex of anesthetized rats. We found that predictably was not static; it depends on cortical state and the duration of prediction. Second, we implemented a closed-loop feedback control to control the neural activity in the motor cortex of anesthetized mice. We found a trade-off between the accuracy and cost of control as we tuned the cortical state with anesthetic drugs. Finally, we studied how single neuron is related to summed activity of large population, referred to as population coupling. We found different neurons within the same network can have diverse population coupling and that this coupling change if we manipulate inhibitory signaling in the network.

Table of contents

List of publications

State-dependent intrinsic predictability of cortical network dynamics, L Fakhraei, SH Gauntam, WL Shew, PLoS one 12 (5), e0173658, Chapter 1, Published.

Introduction

Making sense of brain's complexity is one of the most challenging field of research in modern science. The brain is the most complex organ of the human body and is made up of different regions. The cerebral cortex, located in the outer-most layer of the brain, is the largest region of brain. The cortex plays a key role in many functions including cognition, awareness, thought and language. Although much of traditional neuroscience research has focused on how the cortex processes sensory input or generates motor output, the cortex is continuously processing and computing even without sensory input or body movements. This internal cortical neural activity that is not directly related to sensory input or motor output is often referred to as 'intrinsic', 'spontaneous', or 'ongoing activity'. In general, a complete view of cortical dynamics must account for the interaction of external processes, like sensory stimulation and motor actions, with the intrinsic spontaneous activity. Because the cortical activity is driven as much by spontaneous activity as sensory input in neural processing, understanding of spontaneous activity and cortical states is essential. The work in this thesis is aimed at gaining better understanding of multiple aspects of ongoing cortical dynamics.

The character of ongoing cortical dynamics is highly nonstationary. For example, at sometimes, ongoing cortical dynamics are strongly coordinated with many neurons firing together in synchrony, while at other times the neurons fire more independently. These changes are referred to as changes in 'cortical state'. The cortex continuously alters its internal state depending on changes in the behavior of the organism. One underlying mechanism that is thought to be important for changes in cortical state is the 'balance of excitation and inhibition'. This refers to the ongoing competitive interactions between two types of neurons in the cortex: excitatory neurons, which generate signals that excite other neurons, and inhibitiory neurons, which

generate signals that make other neurons less excited. Here, we manipulated the balance of excitation and inhibition pharmacologically, either with drugs that specifically target inhibitory synapses or with anesthetic drugs, which cause more complex changes in the balance of excitation and inhibition.

We use these manipulations to change the dynamical state of the neuronal population, i.e. to change the 'cortical state'. We did three different studies which ask three different questions about how changes in cortical state impact cortex function.

First we studied how changing cortical states changes temporal continuity and predictability of neuronal network dynamics in experiments with anesthetized rats and in a computational model. We showed that the collective population-level electrical signals, called 'local field potential' (LFP), can be predicted for short periods based on its own history using a simple autoregressive model, but that the efficacy of prediction depended sensitively on the cortical state and how far into the future the prediction was attempted.

Second, we developed a closed-loop feedback control system to try to control the activity in motor cortex of mice. We tuned the cortical state by changing anesthesia and measured how controllability of the neural network depends on cortical state in both experiments and in a computational model. We found a trade-off between the accuracy and cost of control in both experiment and network level computational model.

Finally, we studied how single neurons in motor cortex of awake rats are related to overall firing of the cortical neural population. We asked the question: do all neurons participate with the population in the same way, or are some neurons more strongly 'coupled' to the population than others. We found that population coupling varied greatly from neuron to neuron, from strongly

coupled to weakly coupled neurons. Furthermore we found that manipulation of inhibition changes the population coupling of a neuron.

The results from these three projects provided new fundamental understanding of how changes in cortical state can cause changes in how the cortex works.

Chapter 1

Abstract

The information encoded in cortical circuit dynamics is fleeting, changing from moment to moment as new input arrives and ongoing intracortical interactions progress. A combination of deterministic and stochastic biophysical mechanisms governs how cortical dynamics at one moment evolve from cortical dynamics in recently preceding moments. Such temporal continuity of cortical dynamics is fundamental to many aspects of cortex function but is not well understood. Here we study temporal continuity by attempting to predict cortical population dynamics (multisite local field potential) based on its own recent history in somatosensory cortex of anesthetized rats and in a computational network-level model. We found that the intrinsic predictability of cortical dynamics was dependent on multiple factors including cortical state, synaptic inhibition, and how far into the future the prediction extends. By pharmacologically tuning synaptic inhibition, we obtained a continuum of cortical states with asynchronous population activity at one extreme and stronger, spatially extended synchrony at the other extreme. Intermediate between these extremes we observed evidence for a special regime of population dynamics called criticality. Predictability of the near future (10-100 ms) increased as the cortical state was tuned from asynchronous to synchronous. Surprisingly, predictability of the more distant future (>1 s) was highest for asynchronous states. These experimental results were confirmed in a computational network model of spiking excitatory and inhibitory neurons. Our findings demonstrate that determinism and predictability of network dynamics depend on cortical state and the time-scale of the dynamics.

Significance statement

Many cognitive functions require well-controlled, predictable evolution of brain activity over a period of time. For instance, in working memory tasks we routinely maintain some information "in mind" for a few seconds. On faster timescales, some complex motor tasks are thought to require a nearly deterministic, stereotyped sequence of neural commands to the muscles. What factors affect our ability to carry out such tasks? More generally, what factors affect the temporal continuity and predictability of neural dynamics in the cortex? Our experiments and computational model show that predictability depends strongly on how synchronized the collective dynamics of neurons are. Stronger synchrony results in more predictable dynamics at short time scales, while asynchronous dynamics are more predictable at longer times.

Introduction

Concepts like "train of thought" or "stream of consciousness" evoke a picture of ongoing brain function in which thoughts at one moment are inextricably linked with those of the recent past. The neural underpinnings of such temporal continuity of brain activity are unclear. At a basic physiological level, it is clear that the action potentials at one moment are caused by those occurring in the recent past, which in turn, were caused by earlier neural activity. However, the synaptic interactions that mediate such temporal evolution of neural activity can be strongly modulated, resulting in qualitatively diverse states of neural dynamics, depending on behavioral or pharmacological factors (1, 2). For instance, changes in levels of arousal (3–6), body motility (3), sleep (7), anesthesia (6, 8–10), and the balance of excitation and inhibition (11) can incur dramatic changes in dynamics in cerebral cortex. In this context, it stands to reason that, the

5

temporal continuity of neural activity should depend on the cortical state. To test this hypothesis, we measured how well cortical population activity can be predicted based on its own recent history. We interpret the degree of predictability as a quantitative proxy for the degree of temporal continuity. We experimentally measured ongoing population neural activity in the cortex (multi-site local field potential) and in a computational model network of spiking excitatory and inhibitory neurons. We measured predictability across a continuum of different cortical states incurred, in part, by tuning synaptic inhibition. The continuum of states ranged from asynchronous, weakly correlated activity to strongly fluctuating, synchronous activity. Confirmed by our experiments and our model, we found that predictability does indeed exhibit a complex dependence on cortical state. For short term predictions (<50 ms) asynchronous cortical states were less predictable than synchronous states. Surprisingly, the reverse was true for longer term predictions (> 1s) – the synchronous state was less predictable than the asynchronous state. Together, our experimental and computational results suggest that temporal continuity of ongoing cortical activity can be dramatically altered by tuning inhibitory synaptic interactions or by other means of tuning the cortical state.

Results

We studied temporal continuity and predictability of neuronal network dynamics in experiments and in a computational model. In experiments, we recorded multi-unit activity (MUA) and local field potential (LFP) in somatosensory cortex of anesthetized male rats using 32-channel micro-electrode arrays (Fig 1). Our model consisted of 2952 spiking neurons – 80% excitatory, 20% inhibitory – placed on a two-dimensional grid with spatially localized connectivity. The model neuron dynamics were simulated using established computationally efficient methods (12). Model

6

spiking activity was compared with experiment MUA. Experimental measurements of LFP were compared with the average membrane potential of groups of model neurons (32 groups, akin to the 32 electrodes in experiments, each group was comprised of 81 neurons in a 9 x 9 grid). In the following results, we will first describe how we imposed changes in cortical state and how we quantitatively assess such changes. Second, we will describe how we measure predictability and how predictability depends on cortical state.

In both the experiments and in the model, we manipulated inhibitory synapses to change the dynamical state of the neuronal population. In experiments, inhibition was manipulated pharmacologically with $GABA_A$ agonist muscimol or antagonist bicuculline. Moreover, in experiments, the dynamical state exhibited changes without direct experimental control, likely due to changes in anesthetic depth. Our data analysis accounts for both the naturally occurring shifts in state and the pharmacologically induced shifts, as we describe further below. In both the experiment and the model, we found that enhanced inhibition resulted in asynchronous, low rate population activity, while reduced inhibition typically resulted in large bursts of correlated activity (Fig1)
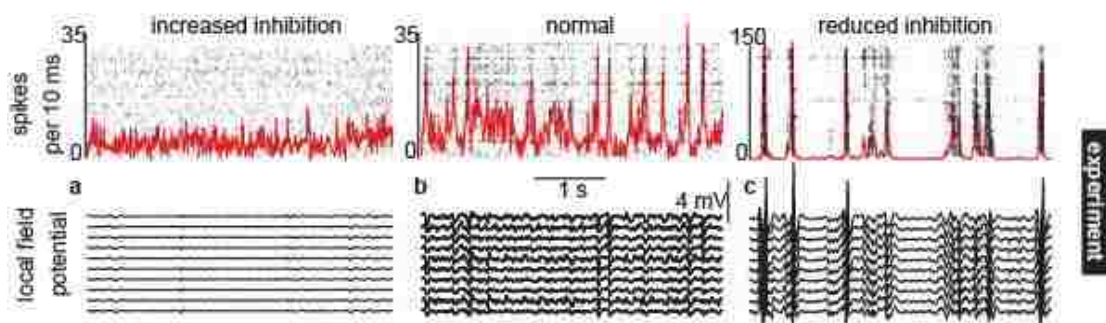
Fig 1) Tuning inhibition to alter the cortical state. we studied a range of cortical states characterized at one extreme by asynchronous firing and low amplitude LFP (a) and at the other extreme by firing synchrony and large amplitude LFP (c). These extremes were typically observed when inhibition was increased or decreased, respectively. In between the extremes, population spiking was more varied and LFP was moderate in amplitude (b).

7
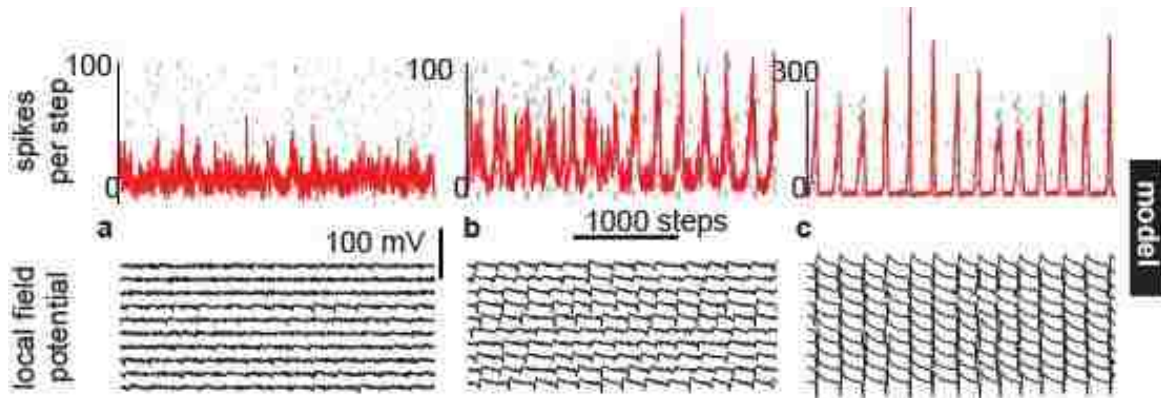
Fig 2) The same as Fig 1 except the shown model examples were computed with *IC*=-75 (increased inhibition), *IC*=-28.5 (normal), and *IC*=-7.5 (reduced inhibition).

We quantitatively assessed changes in the dynamical state of the network based on the prevalence of different spatiotemporal scales of population activity. More specifically, we analyzed distributions of 'avalanche' sizes. An avalanche is a period of elevated population activity, which we defined based on MUA spike count time series for the entire population, as other in recent studies (13–15). In brief, an avalanche is defined as an excursion above a threshold level of spiking. The size of an avalanche is defined as the total number of spikes that occur during this period of above-threshold activity. Distributions of avalanche sizes reveal how often large avalanches occur relative to small avalanches, thus assessing the prevalence of different spatiotemporal scales of population activity (Fig 2a, d).

Fig 3) Parameterizing the experimental cortical state based on avalanche distributions. For both the experiment (a-c), we indexed the continuum of observed cortical states based on the prevalence of different spatiotemporal scales of activity. **a)** Each line shows one probability density distribution of avalanches obtained from one 20 min experimental recording of ongoing activity (shifted vertically to faci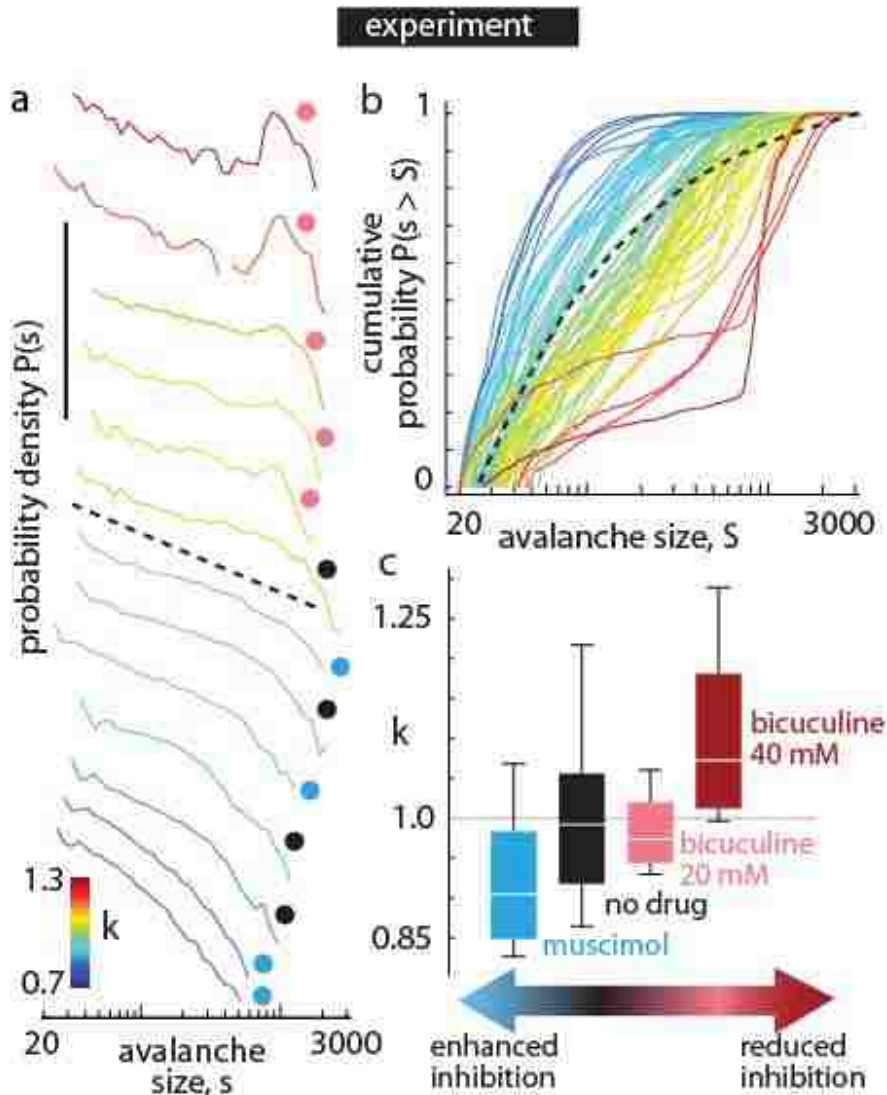litate comparison of the distribution shapes). Both vertical and horizontal axes are logarithmic. Vertical scale bar indicates 5 orders of magnitude. The colored dot beside each distribution indicates the experimental drug condition (black – no-drug; blue – muscimol; pink – bicuculline 20 μM). A subset of all experiments is shown. Line color indicates the κ value, which measures deviation from a power-law distribution with exponent -1.5 (black dashed line). When large bursts of population activity are dominant $\kappa > 1$ and when large bursts are absent $\kappa < 1$. **b)** The probability distributions shown in panel (a) are shown here as cumulative distributions. Color indicates κ, which is defined as the mean of 10 differences (equally spaced across the horizontal axis) between the measured distributions and the reference power-law distribution (black dashed). One distribution for each experiment is shown. **c)** Shown are the upper and lower quartiles, median, and range (box bottom, top, midline, and error bars, respectively) of κ values

9

for each drug condition. Note that decreasing or increasing inhibition systematically increases or decreases κ, respectively.
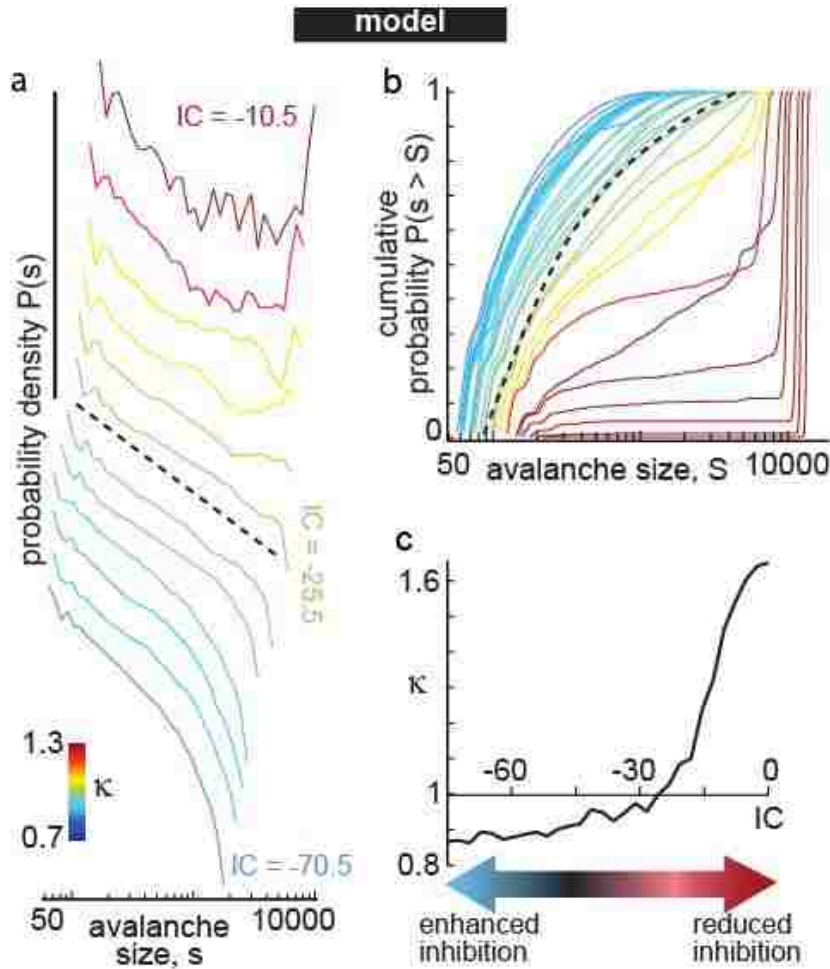
Fig 4) Parameterizing the model cortical state based on avalanche distributions. a-c) The model results closely parallel the experimental findings. In the model, we treat the pharmacological changes by directly tuning the strength of inhibitory connections (*IC*). Tuning *IC* in the model results in the same family of avalanche size distributions as seen in the experiments.

A convenient parameter to index the continuum of observed cortical states, called κ, was developed in previous studies of neuronal avalanches (13, 16, 17). Based on cumulative probability distributions (Fig 2b, e) κ quantifies how an observed avalanche size distribution deviates from a -1.5 power law. When κ was less than 1, large avalanches were rare and the size distribution was

10

close to exponential in form. When κ was greater than 1, large avalanches were dominant, typically exhibiting a bimodal distribution of sizes. Intermediate between these extremes, avalanches occurred with diverse sizes and the size distribution had a form close to a power law with exponent -1.5. By definition, a perfect match to -1.5 power law corresponds to κ=1. Importantly, κ allows quantitative comparison of experimental and model results, because κ is readily obtained from both.

In our model, κ≈1 occurred uniquely near the boundary between two different regimes in parameter space. This observation is in line with the possibility that our model undergoes a phase transition as inhibition is tuned from strong to weak. Indeed, a power law avalanche size distribution with -1.5 exponent is often cited as evidence that the system operates in a special dynamical regime, called criticality (18, 19), which is expected to occur at the tipping point of such a phase transition. To our knowledge, our model has not been used to study critical phenomena previously. Nonetheless, our model results are consistent with previously studied models, in which inhibition can serve as a control parameter for a phase transition (15, 20–22).
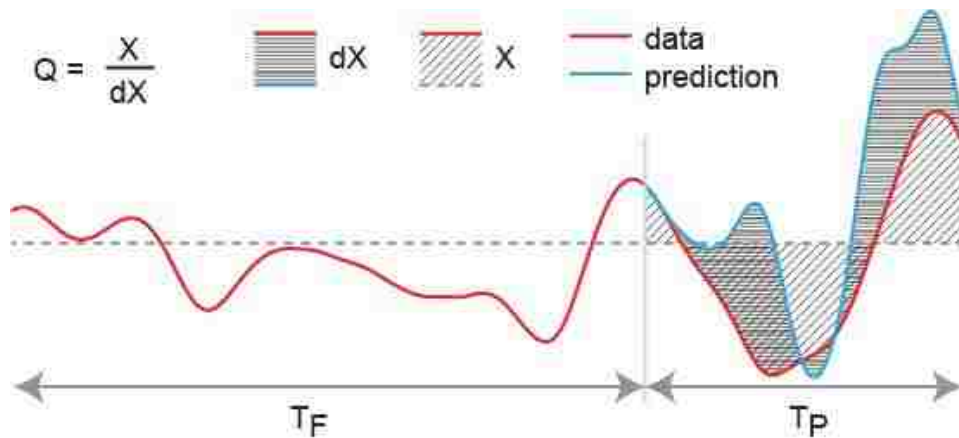
Fig 5) Measuring predictability of multisite LFP. We fit an autoregressive model to a period of recorded data of duration T_f. This fit is based on all 32 channels, even though only one channel is shown here. We predict a period of duration T_p following the fitting time window. The prediction (blue) is compared with the true measured data (red) to assess the efficacy of the prediction Q.
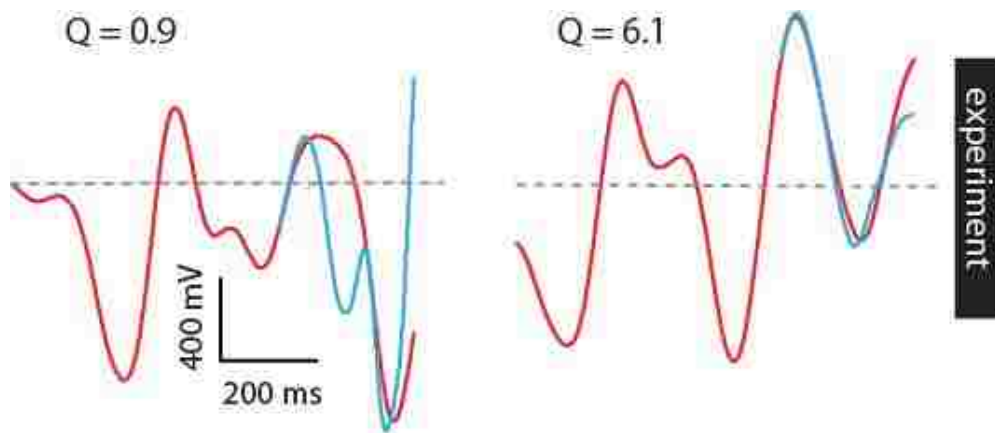
Fig 6) Examples for prediction in the experiment. Shown are examples of a poor prediction from the experiment(a), a good prediction from the experiment (b).
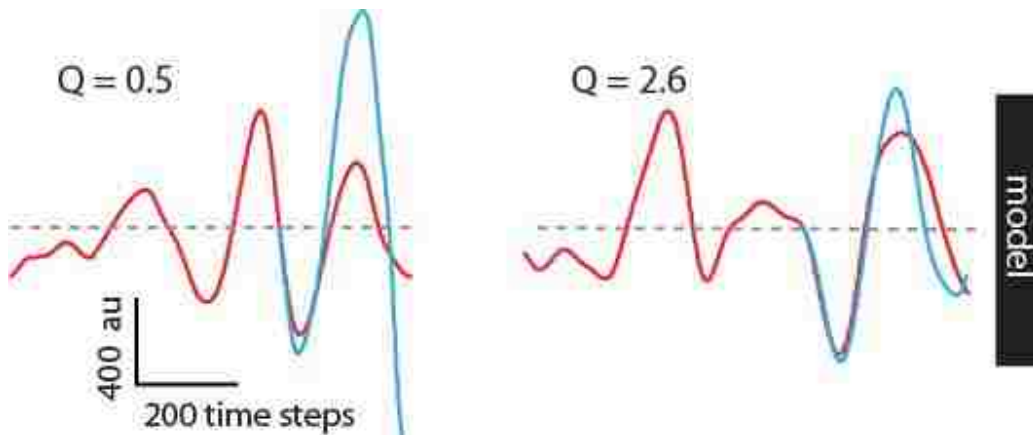
Fig 6) Examples for prediction in the model. Shown are examples of a poor prediction from the model, b) and a good prediction from the model (b).
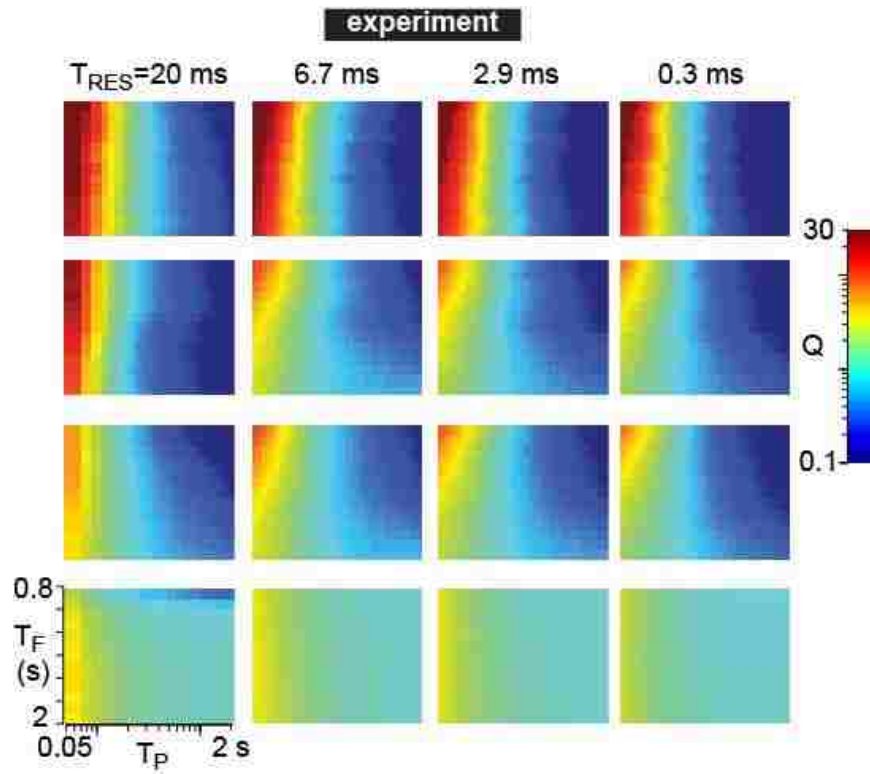
Fig 7) Predictability depends on time scales for experimental LFP. Here we show how predictability Q (color) depends on the fitting time T_f, the prediction time T_p, time resolution of the recording T_{RES}, and frequency band of filtering. The example is from a no-drug recording with $\kappa=0.99$.
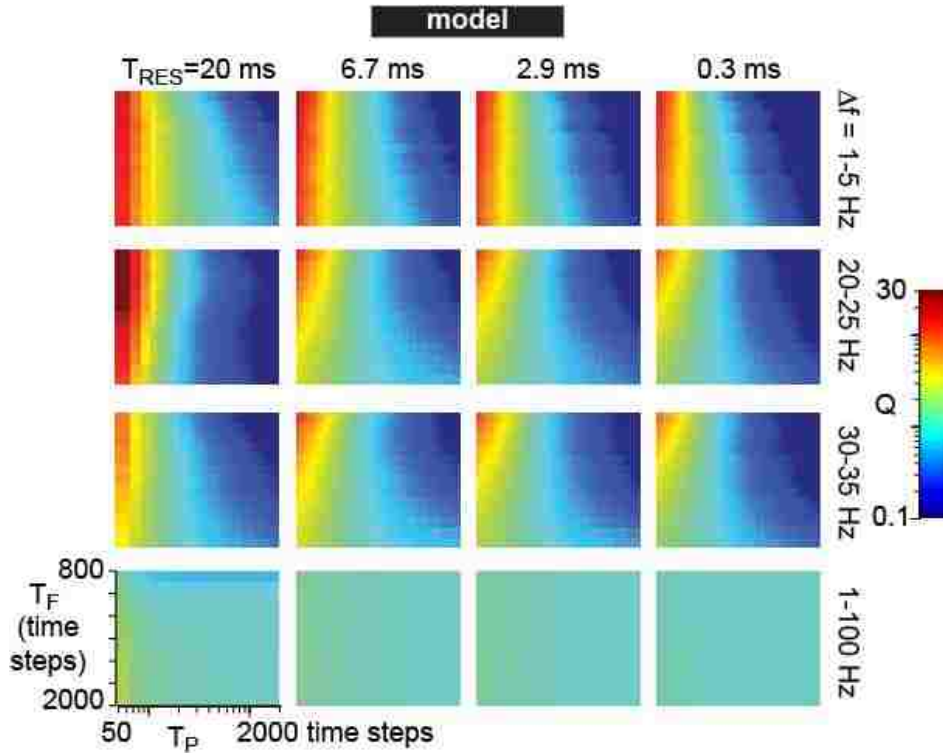
Fig 8) Predictability depends on time scales for model LFP. The same as Fig 7 except The example model was simulated with IC=-30 and κ=0.95. We find good agreement between the experiment and model. Predictions are more sensitive to changes in T_P than T_F. Low frequencies are more predictable than high frequencies for small T_P, while the opposite is true for longer T_P.

To determine how the temporal continuity of cortical population dynamics depends on cortical state changes, i.e. changes in κ, we next computed the predictability of population dynamics. We computed predictions of many short periods of ongoing activity and averaged them to assess the overall predictability Q of a given recording. The first step in computing a prediction was to fit an autoregressive model to a short duration T_F of local field potential (LFP) recorded from 32 electrodes (Fig 3a), similar to other recent studies (9, 23). After fitting the autoregressive model, it was used to predict LFP during a short time window T_P immediately following the fitting time window (Fig 3a). An autoregressive model is meant to handle continuous variables, and thus, is a natural choice for assessing predictability of LFP. Although an autoregressive model is a linear

14

model, and cortical dynamics are certainly nonlinear, it is expected that, over sufficiently short times, nonlinear dynamics can be well approximated by a linear model. Indeed, our predictions were often quite high in quality for short time periods (Fig 3c, e and Fig 4). However, we do not know *a priori* what duration is sufficiently short for such a linear approximation to be accurate. Indeed, as we will show below, the efficacy of such linear modeling can depend sensitively on changes in cortical state. Rather than pick a single time period T_P, we studied a range of time windows T_P from 50 ms to 2 s. We also examined a range of fitting time window durations T_F from 0.8 to 2 s. As expected, shorter times were much more predictable than longer times, i.e. prediction quality Q was highest for short T_P; Q also depended on T_F, but not as strongly as it depended on T_P (Fig 4). We also note that the prediction is more effective in restricted frequency bands, compared to broadband LFP (Fig 4), generally slow frequencies (1-5 Hz) were most accurately predicted. Moreover, the time resolution of the data (i.e. the sample rate) can also significantly influence predictability (Fig 4). Generally, we found that predictability depended on T_P, T_F, frequency band, and time resolution in a similar way for the experiment (Fig 4a) and the model (Fig 4b).

Finally, we determined how predictability depends on the cortical state, i.e. how Q depends on κ for broadband LFP (1-100 Hz) both in the experiment and the model (Fig 5). In our experiments, we found that for short time predictions (small T_P), Q rises gradually as κ is increased from 0.7 to near 1 and then increases more sharply for $\kappa > 1$. For longer time predictions (large T_P), we were surprised to find precisely the opposite trend; Q falls gradually as κ is increased from 0.7 to near 1 and then decreases more rapidly for $\kappa > 1$. These data demonstrate that the highly synchronous state with $\kappa > 1$ is relatively difficult to predict at long times, but quite predictable at short times. This variability in predictability across timescales is less dramatic for asynchronous cortical states

with κ<1. Moreover, the mean predictability across timescales is highest in the synchronous state and lowest in the asynchronous state. A balance is found for intermediate states with κ~1; the mean predictability is not too low, and the variability in predictability is not too high. These experimental results were in good agreement with our model results, but the model allowed us to extend the range of κ values to higher values. For these extremely synchronous states, the model revealed a drop in predictability for the highest κ values (κ>1.3) even for short time predictions.
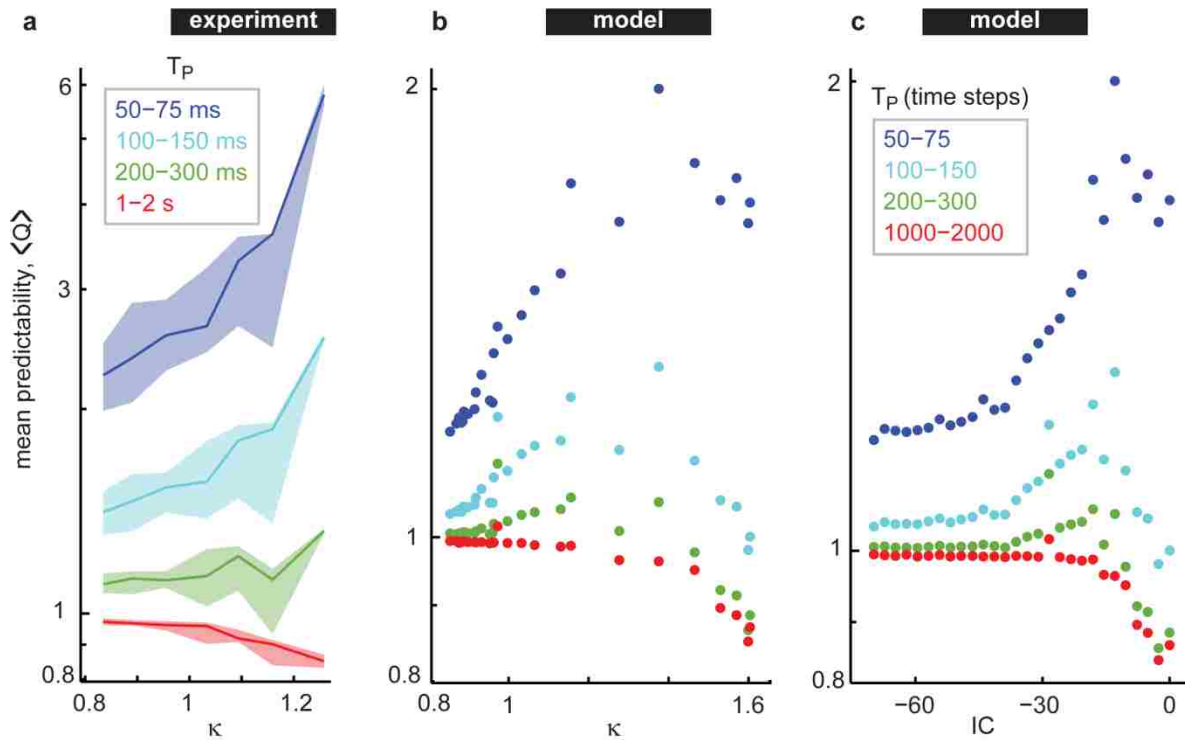
Fig 5) Time-dependent reversal of predictability vs. cortical state. a) For short-term predictions (T_P=10-100 ms, purple), mean predictability rises as the cortical state is tuned from asynchronous to synchronous, i.e. for increasing κ. For longer-term predictions (T_P=1-2 s, red), this trend reverses; low κ is more predictable than high κ. Each curve summarizes data from all experiments (n=72). Line indicates the median. Shaded region delineates quartiles. Vertical axes are logarithmic. **b)** We observed the same trend in the model for the experimentally observed range of states (0.8 > κ > 1.3). For more extremely synchronous states (κ > 1.3) the model revealed a decline in predictability for all prediction durations. **c)** The model data predictability values are shown versus inhibitory synapse strength *IC*. The <Q> values in this figure (all panels) represent an average of Q over all T_F, all T_{RES}, and a range of T_P for each dataset.

Materials and Methods

Electrophysiology

All procedures were carried out in accordance with the recommendations in the Guide for the Care and Use of Laboratory Animals of the National Institutes of Health and approved by University of Arkansas Institutional Animal Care and Use Committee (protocol #12025). We studied adult male rats (n=12, 328±54 g; Rattus Norvegicus, Sprague-Dawley outbred, Harlan Laboratories, TX, USA). Anesthesia was induced with isoflurane inhalation and maintained with urethane (1.5 g/kg body weight (bw) dissolved in saline, intraperitoneal injection (ip)). Dexamethasone (2 mg/kg bw, ip) and atropine sulphate (0.4 mg/kg bw, ip) were administered before performing a 2 mm x 2 mm craniotomy over barrel cortex (1 to 3 mm posterior from bregma, 5 to 7 mm lateral from midline).

Extracellular voltage was recorded using 32-channel microelectrode arrays (8 shanks, 4 electrodes/shank, 200 μm inter-electrode distance, 400 μm inter-shank distance, A468-5mm-200–400-177-A32, NeuroNexus, MI, USA). Insertion depth was 650 μm, centered 2 mm posterior from bregma and 6 mm lateral from midline. Voltages were measured with respect to an AgCl ground pellet placed in the saline-soaked gel foams, which protect the exposed tissue surrounding the insertion site. Voltages were digitized with 30 kHz sample rate (Cereplex + Cerebus, Blackrock Microsystems, UT, USA). Recordings were filtered between 300 and 3000 Hz and thresholded at -3 SD to detect multi-unit activity (MUA).

Pharmacology

Six 20 min recordings were conducted with each rat. First, three recordings were performed with no direct manipulation of inhibition (n=36, indirect effects may be imposed by anesthetics (35) and atropine sulfate). Then, three recordings were performed with a drug topically applied via gel foam pieces soaked in saline mixed with drug. Three drug conditions were studied (one condition per rat): 1) 20 μM muscimol (6 rats, 18 recordings), 2) 20 μM bicuculline methiodide (3 rats, 9 experiments), 3) 40 μM bicuculline methiodide (3 rats, 9 experiments).

Avalanche definition

We define an avalanche based on the spike count time series $c(t)$ of MUA recorded on all electrodes, counting spikes in consecutive 15 ms time bins. An avalanche begins at t_i when $c(t_i)$ exceeds a threshold equal to the mean spike count. The avalanche ends at t_f when $c(t_f)$ drops back below the threshold. The avalanche size s is defined as the total number of spikes occurring between t_i and t_f, $s = \sum_{n=i}^{f} c(t_n)$. Our approach for defining avalanches contrasts with many previous studies of neuronal avalanches, which were mostly based on local field potential. A few other experimental studies have considered spike avalanches, but defined the start and stop of avalanches as time periods with no spiking (36, 37). In our view, this previous definition is inherently limited, because it does not scale well with increasing numbers of measured neurons and does not account for the fact that some neurons fire at extremely high rates. Moreover, it may be the case that the cortex operates in a regime with inherently self-sustained ceaseless dynamics, as studied in recently in the context of avalanches (14). In this case, it does not make sense to define avalanches based on quiet periods with no spiking, because such quiet periods do not exist.

As tools for measuring large populations of neurons become more prevalent, it is likely that a well-sampled population of neurons in real cortex will also be devoid of meaningful silent periods.

κ parameter

Deviation from the reference power-law (-1.5 exponent) was quantified with κ, which is a previously developed non-parametric measure with similarities to a Kolmogorov-Smirnov statistic (17, 24); κ equals 1 plus the sum of 10 differences (logarithmically spaced) between the observed avalanche size distribution (recast as a cumulative distribution) and a perfect power-law with exponent -1.5 (in cumulative form).

Computational model

Our model consisted of 2952 spiking neurons – 80% excitatory, 20% inhibitory – placed on a 72 x 36 grid (the 2:1 aspect ratio matched the geometry of the experimental electrode arrays). Each neuron was modeled with two coupled differential equations which were derived from the Hodgkin–Huxley equations by Izhikevich (12),

$$\frac{dv_i}{dt} = 0.04v_i^2 + 5v_i + 140 - u_i + I_i \quad \text{and} \quad \frac{du_i}{dt} = a(bv_i - u_i),$$

where v_i represents the membrane potential of neuron i and u_i represents the 'recovery' variable of neuron i. The parameter a represents a scale time of recovery and b couples the membrane potential and recovery potential. For all excitatory neurons, $a = 0.02$ and $b = 0.2$. For inhibitory neurons a and b are drawn from uniform distributions on [0.02, 0.1] and [0.2, 0.25], respectively. When the membrane potential v_i exceeds 30, the neuron fires. Upon firing, v_i is reset to -65 and

u_i is incremented to $u_i + d$, where d is 2 for all inhibitory neurons and drawn from a uniform distribution on [2, 8] for excitatory neurons. We use the numerical techniques developed by Izhikevich (12) to simulate these dynamics.

The input I_i to neuron i is comprised of random external input η and input due to presynaptic firing of the other neurons in the model,

$$I_i(t) = \eta_i(t) + \sum_{j=1}^{N} S_{ij} x_j(t-1)$$

where η is drawn from a uniform distribution with mean 3 and unity standard deviation. Here $x_j(t)$ is a binary variable equal to one when neuron j fires and zero otherwise. The synapse from neuron j to neuron i is represented by the connection matrix element S_{ij}. The S matrix was constructed in three steps. First, for excitatory presynaptic neurons, S_{ij} is drawn from a normal distribution with mean 8.4 and standard deviation 1.5. Second, for inhibitory presynaptic neurons, S_{ij} is drawn from a normal distribution with mean IC and standard deviation 1.5. To model the experimental pharmacological manipulation of inhibitory interactions we studied 30 different values of IC linearly spaced between -75 and 0. Finally, long-range connections were attenuated, by multiplying all S_{ij} by a distance dependent factor $e^{-d_{ij}^2/d_0^2}$, where $d_0 = 2.24$ and d_{ij} is the distance between neuron i and neuron j. For each IC, the model was run for 500000 time steps (500 s, considering 1 time step to be 1 ms).

Model LFP

To derive an LFP-like variable from our model dynamics we divided the 2D grid into 32 equal groups (each 9 x 9 in model grid space) meant to represent the 32 electrode channels in our experiments. To obtain the LFP for each group, we computed the average v_i across all neurons within the group, in line with experiments that show a close relationship between membrane potential fluctuations and LFP (38). We clipped spikes before this averaging process. Finally, we filtered the model LFP just as we did with the experimental data.

Auto regressive model fitting and prediction

We use a first order autoregressive model to generate the predictions reported here. The model specifies how each single LFP channel at time t, $y_i(t)$, is determined by all other LFP channels at previous times

$$y_i(t) = \sum_{j=1}^{n} A_{ij} y_j(t-1) + \epsilon(t),$$

where n is the number of LFP channels (32 in our experiments and model) and t is a discrete variable advancing 1 per sample. A is a 32 x 32 matrix which specifies how each channel influences each other channel and ϵ is a noise term. The matrix A and the noise ϵ are determined by fitting this model to a short period T_f of recorded data. For the fitting procedure, we used the Neumaier and Schneider (2001) algorithm implemented with the 'ARfit' functions developed by Tapio Schneider for Matlab (Mathworks) (39). After obtaining the best fit *A* based on the period starting at time t and ending at time *t+T_f*, we then constructed a prediction over a time period with duration T_p starting at time *t+T_f+1*. The prediction is constructed by iteratively applying the above equation starting with $y(t + T_f + 1)$ as an initial condition.

21

Conclusion

Here we measured multisite ongoing population activity in anesthetized rat somatosensory cortex. We showed that LFP can be predicted for short periods based on its own history using a simple autoregressive model, but that the efficacy of prediction depended sensitively on the cortical state and how far into the future the prediction was attempted. Based on distributions of population activation events, called neuronal avalanches, we parameterized a continuum of cortical states ranging from asynchronous, weakly correlated activity to large-scale synchronous activity. We found that near future (~10-100 ms) predictability is lower for the weakly correlated end of the continuum compared to synchronous states. This trend reverses for longer term predictions (~1 s); the synchronous state was less predictable than the asynchronous state. We observed a similar continuum of states and relationship between predictability and state in a network model of spiking neurons.

We parameterized the continuum of observed cortical states using κ, which measures how the avalanche size distribution deviates from a power law with exponent -1.5, as in previous studies (13, 17, 24, 11, 15). Such power law distributed avalanches are predicted to occur at the critical point of a phase transition (25–27). The hypothesis that cortical network dynamics can be tuned through a phase transition has a long history with origins in statistical physics research and, more recently, growing support from neuroscience experiments (17, 28–32). Near the 'center' of our observed continuum of cortical states, we found $\kappa \approx 1$, i.e. avalanche size distributions that were close to power law in form. This observation suggests that the continuum of cortical states we observed spans a critical phase transition, both in the experiment and the model. In this context, our observations suggest that, for both short and long time scales, criticality marks the tipping point between low to high predictability. However, which way the predictability tips, toward high

or low values, depends on the time scale of prediction. Although many types of phase transitions can occur in different systems, all can be characterized as a transition between an ordered phase and a disordered phase. In the context of our findings, the disordered phase corresponds to the asynchronous, low kappa end of the cortical state continuum. The ordered phase corresponds to the synchronous, high kappa end of the continuum. From this point of view, it is perhaps not surprising that the ordered phase is more predictable than the disordered phase, as we see for the short term predictions. However, the drop in predictability in the ordered phase for longer time scales is more surprising.

One limitation of our work is that the continuum of cortical states was observed in anesthetized animals. Thus, it remains for future experiments to test whether a similar continuum of cortical states and corresponding predictability exists during wakefulness. This possibility is plausible, because previous studies have demonstrated behaviorally relevant changes in κ. For example, EEG recordings in humans suggest that sleep deprivation can elevate κ (33), while increased attention to a reaction time task can decrease κ (34). Another study has shown that as a mouse awakens following pentobarbital anesthesia, κ decreases from values typically >1 to values closer to 1 as the arousal increases (17). In this context, our results predict that the extremes of predictability, either high or low, are avoided in the awake state. We anticipate that future experiments will provide answers to these interesting questions.

References

1.   Harris KD, Thiele A (2011) Cortical state and attention. *Nat Rev Neurosci* 12:509–23.

2.   Renart A, Machens CK (2014) Variability in neural activity and behavior. *Curr Opin Neurobiol* 25C:211–220.

3.   Vinck M, Batista-Brito R, Knoblich U, Cardin JA (2015) Arousal and Locomotion Make Distinct Contributions to Cortical Activity Patterns and Visual Encoding. *Neuron* 86:740–754.

4.   Favero M, Varghese G, Castro-Alamancos MA (2012) The state of somatosensory cortex during neuromodulation. *J Neurophysiol* 108:1010–24.

5.   Goard M, Dan Y (2009) Basal forebrain activation enhances cortical coding of natural scenes. *Nat Neurosci* 12:1444–9.

6.   Bermudez Contreras EJ et al. (2013) Formation and reverberation of sequential neural activity patterns evoked by sensory stimulation are enhanced during cortical desynchronization. *Neuron* 79:555–66.

7.   Steriade M (2003) *Neuronal Substrates of Sleep and Epilepsy* (Cambridge University Press, Cambridge).

8.   Ching S, Brown EN (2014) Modeling the dynamical effects of anesthesia on brain circuits. *Curr Opin Neurobiol* 25C:116–122.

9.   Solovey G et al. (2015) Loss of Consciousness Is Associated with Stabilization of Cortical Activity. *J Neurosci* 35:10866–10877.

10.   Alkire MT, Hudetz AG, Tononi G (2008) Consciousness and anesthesia. *Science* 322:876–80.

11.   Shew WL, Yang H, Yu S, Roy R, Plenz D (2011) Information Capacity and Transmission

Are Maximized in Balanced Cortical Networks with Neuronal Avalanches. *J Neurosci* 31:55–63.

12. Izhikevich EM, Izhikevich EM (2003) Simple model of spiking neurons. *IEEE Trans Neural Netw* 14:1569–72.

13. Poil S-S, Hardstone R, Mansvelder HD, Linkenkaer-Hansen K (2012) Critical-state dynamics of avalanches and oscillations jointly emerge from balanced excitation/inhibition in neuronal networks. *J Neurosci* 32:9817–23.

14. Larremore DB, Shew WL, Ott E, Sorrentino F, Restrepo JG (2014) Inhibition Causes Ceaseless Dynamics in Networks of Excitable Nodes. *Phys Rev Lett* 112:138103.

15. Gautam SH, Hoang TT, McClanahan K, Grady SK, Shew WL (2015) Maximizing Sensory Dynamic Range by Tuning the Cortical State to Criticality. *PLOS Comput Biol* 11:e1004576.

16. Shew WL, Yang H, Petermann T, Roy R, Plenz D (2009) Neuronal avalanches imply maximum dynamic range in cortical networks at criticality. *J Neurosci* 29:15595–600.

17. Scott G et al. (2014) Voltage Imaging of Waking Mouse Cortex Reveals Emergence of Critical Neuronal Dynamics. *J Neurosci* 34:16611–16620.

18. Plenz D, Niebur E, Schuster HG (2014) *Criticality in Neural Systems* eds Plenz D, Niebur E, Schuster HG (Wiley, Weinheim, Germany).

19. Shew WL, Plenz D (2013) The functional benefits of criticality in the cortex. *Neuroscientist* 19:88–100.

20. Wang S-J, Hilgetag CC, Zhou C (2011) Sustained activity in hierarchical modular neural networks: self-organized criticality and oscillations. *Front Comput Neurosci* 5:30.

21. Larremore DB, Shew WL, Ott E, Sorrentino F, Restrepo JG (2013) Inhibition causes

ceaseless dynamics in networks of excitable nodes. 5.

22.   Yang H, Shew WL, Roy R, Plenz D (2012) Maximal Variability of Phase Synchrony in Cortical Networks with Neuronal Avalanches. *J Neurosci* 32:1061–1072.

23.   Solovey G, Miller KJ, Ojemann JG, Magnasco MO, Cecchi G a (2012) Self-Regulated Dynamical Criticality in Human ECoG. *Front Integr Neurosci* 6:44.

24.   Shew WL, Yang H, Petermann T, Roy R, Plenz D (2009) Neuronal Avalanches Imply Maximum Dynamic Range in Cortical Networks at Criticality. *J Neurosci* 29:15595–15600.

25.   Larremore DB, Carpenter MY, Ott E, Restrepo JG (2012) Statistical properties of avalanches in networks. *Phys Rev E* 85:066131.

26.   Harris TE (1963) *The Theory of Branching Processes* (Springer-Verlag, Berlin).

27.   Muñoz M, Dickman R, Vespignani A, Zapperi S (1999) Avalanche and spreading exponents in systems with absorbing states. *Phys Rev E* 59:6175–6179.

28.   Shew WL et al. (2015) Adaptation to sensory input tunes visual cortex to criticality. *Nat Phys* 11:659–663.

29.   Bellay T, Klaus A, Seshadri S, Plenz D (2015) Irregular spiking of pyramidal neurons organizes as scale-invariant neuronal avalanches in the awake state. *Elife* 4:1–25.

30.   Beggs JM, Plenz D (2003) Neuronal avalanches in neocortical circuits. *J Neurosci* 23:11167–77.

31.   Haimovici A, Tagliazucchi E, Balenzuela P, Chialvo DR (2013) Brain Organization into Resting State Networks Emerges at Criticality on a Model of the Human Connectome. *Phys Rev Lett* 110:178101.

32. Petermann T et al. (2009) Spontaneous cortical activity in awake monkeys composed of neuronal avalanches. *Proc Natl Acad Sci U S A* 106:15921–6.

33. Meisel C, Olbrich E, Shriki O, Achermann P (2013) Fading Signatures of Critical Brain Dynamics during Sustained Wakefulness in Humans. *J Neurosci* 33:17363–17372.

34. Fagerholm ED et al. (2015) Cascades and Cognitive State: Focused Attention Incurs Subcritical Dynamics. *J Neurosci* 35:4626–4634.

35. Populin LC (2005) Anesthetics change the excitation/inhibition balance that governs sensory processing in the cat superior colliculus. *J Neurosci* 25:5903–14.

36. Dehghani N et al. (2012) Avalanche Analysis from Multielectrode Ensemble Recordings in Cat, Monkey, and Human Cerebral Cortex during Wakefulness and Sleep. *Front Physiol* 3:302.

37. Ribeiro TL et al. (2010) Spike Avalanches Exhibit Universal Dynamics across the Sleep-Wake Cycle. *PLoS One* 5:e14129.

38. Okun M, Naim A, Lampl I (2010) The Subthreshold Relation between Cortical Local Field Potential and Neuronal Firing Unveiled by Intracellular Recordings in Awake Rats. *J Neurosci* 30:4440–8.

39. Neumaier A, Schneider T (2001) Estimation of parameters and eigenmodes of multivariate autoregressive models. *ACM Trans Math Softw* 27:27–57.

Chapter 2

Abstract

Closed-loop feedback control approaches allow precise, real-time control of neural activity to lock spiking activity to specific target spiking rate within the neural network. These approaches enable investigators to tune the ongoing brain activity , induce or disrupt the related frequency of neural network in order to achieve better functionality.

Here we implement a continuous, precise closed-loop feedback control to lock the firing rate at specific targeted spiking activities in the motor cortex of isoflurane-anesthetized rats and in a computational network-level model. We found that controllability of neural activity strikingly varies as neural state changes. Furthermore, we found a trade-off between the accuracy of control and energy required to maintain it both in the experiment and computational model.

Introduction

Cortical spontaneous activity

Cortical activity is determined by the interaction of external stimulation and intrinsic spontaneous activity. Because the cortical activity is driven as much by spontaneous activity as sensory input in neural processing, understanding of spontaneous activity and cortical states is essential.

In early studies, relatively low spiking rate and apparent stochasticity of spontaneous activities caused investigators to suspect that spontaneous activities represent noise [1]. But in later studies, a strong correlation between individual cells firing and its neighbor's spontaneous activity was revealed [2],[3], indicating that if spontaneous activity is 'noise', then this noise is not independent from one neuron to another. Other studies revealed that fluctuation of spontaneous population

activity is comparable to average response to a strong stimulus [4],[5], suggesting that it should not be neglected when trying to understand how the cortex processes sensory stimuli. These studies suggested that spontaneous activity has a spatiotemporal structure with a potential role in processing the cortical population activity.

One hypothesis is that the spatiotemporal structure of ongoing cortical activity reflects neural network connectivity. Studies supporting this hypothesis suggest that the spontaneous activity can be used to disclose the complex structure and wiring of the neural network [6].

How important is the functional role of spontaneous activity in neural processing? Could a strong external stimulation wipe out the footprint of cortical ongoing activity prior to the onset of stimuli? In other words, can stimulus overwhelm the intrinsic population activity? Many studies and evidence show that this is not the case [7],[8],[9],[10]. The external stimulation will not suppress the ongoing population activities but interact with them. In fact, the large trail-to-trial variability of response evoked by repeated presentation of identical stimuli can be partially explained by variability of ongoing population activities prior to the presentation of stimuli. It has been shown that linear summation of ongoing background cortical activity and a stereotyped response could reliably predict the response [7].

Cortical state

The statistical structure of cortical spontaneous activity changes depending on the internal brain state. Changes in brain state are often assessed based on measurements of voltage fluctuations using electrodes implanted in the extracellular space. In particular, low frequency (1-100 Hz) voltage fluctuations, called 'local field potential' (LFP) are useful indicators of changes in brain

state.   Although the biophysics underlying LFP signals is very complex and incompletely understood, LFP is known to originate from a sort of aggregate, collective activity of many neurons nearby the measurement location.   Much of the LFP signal seems to originate from dendritic processing of synaptic inputs [11].

Prominent examples of changes in brain state are caused by sleep-wake cycle [12]. In slow wave sleep, low-frequency local field potential (LFP) fluctuations are dominant in the ongoing cortical activity and cortex operates within an inactivated or synchronized state with an ordered and regular pattern. In contrast, cortex operates in an activate or desynchronized state with iregular, disorded and high-frequency local field potential patterns during rapid eye movement (REM) sleep. Recent studies show that the state of cortex changes even with wakefulness, so that during the attention and behavior, low-frequency fluctuations are suppressed and cortical activity pattern shows desynchronization whereas, during quiescence or drowsiness, cortex operates in a synchronized state with low-frequency oscillation [12].

Although the classical picture holds that cortex usually operates within the synchronized state in anesthetized animal, recent studies show that cortex can exhibit either synchronized or desynchronized state under anesthesia, depending on the type of anesthetic and depth of anesthesia. It has been shown that urethane anesthetized animals mimic the spontaneous and sleep-like cycling of the brain during natural sleep [12]. In summary, the cortex can operate in a continuum of states with synchronized and desynchronized state at the two extremes in this continuum [13],[14],[11],[15],[14],[16],[17],[18],[19].

Also, it has been shown that there is a strong correlation between intracellular voltage measurements and population activity; fluctuation of membrane potential changes with internal brain state [20]. During the desynchronization, intracellular voltage reveals a small, fast large-amplitude intracellular fluctuation whereas, during synchronization, it shows a slow, large-amplitude and steady intracellular fluctuation. However, most the work in this thesis is based on LFP measurements, so we will not discuss intracellular measurements any further.

Sensory response and cortical state

Although the response to a sudden sensory stimulus is typically large regardless of background ongoing activity, it varies as cortex alters its internal state between synchronized and desynchronized states. For example, during synchronization and quiescent animal, the initial response (~50ms after the onset of stimuli) to a punctuate stimuli (i.e. an unexpected brief stimuli) are large, while during the desynchronization and active animal, cortex generates a smaller response[21],[22].

State dependency of cortical response for the later response of isolated punctuate stimuli (> 50ms) is more complex. Within the desynchronized state, a punctuate stimuli modulates a brief response accompanied by suppression which lasts ~100ms, while punctuate stimuli evokes a prolonged response with no suppression in the synchronized state [23],[24].

Response to a high-frequency sequence of stimuli also varies as state changes. In the desynchronized state, the first stimulus of the sequence evokes a smaller response but adaptation

to repeated stimuli is weaker compared to a synchronized state so that after some repetition of stimuli, the response of synchronized state is equal or even smaller than the desynchronized state. Why does a quiescent animal evoke a larger response and adaptation comparing to an active and awake animal? There is a hypothesis that when cortex maintains the synchronized state in an anesthetized and quiescent awake animal, synapses are often in resting state so they are electrically less active. Therefore, they can save energy to perform other functions. Also, when the cortex evokes a large response to the first stimulus in a high repetitive stimulus within synchronization, it leaves less energy for response to other stimuli in the train therefore the response would suppress stronger in synchronized than the desynchronized state. [25],[26]

Despite apparent complex state dependency of cortical response, investigators developed a simple excitable model to predict subsequent sensory response using background ongoing activity prior to the presentation of stimuli, they estimated the parameters of the model using spontaneous activity prior to the onset of stimuli. Model dynamics was changed to reproduce different cortical states, a nonlinear, self-exciting system generated synchronized state and a linear system in reproduced desynchronized states.

response to an isolated unattended stimulus was quantitatively predicted on a trial-by-trial basis using a simple dynamical system, it was shown that response is generated based on the same dynamics as spontaneous activity [23].

Closed loop control systems

A closed loop control system, also referred to as a self-adjusting system, is an interdisciplinary branch of engineering that deals with trying to control the output of a system using feedback. The idea is to measure the error or difference between the output of a system and some desired target output and use this error signal to modify the input to the system (figure 1).

In order to maintain a successful control, there must be a mathematical relationship between the measured output and input. Perhaps the most popular example of a closed loop control systems is automobile cruise control which maintains a constant speed by accelerating or decelerating the car to reach a target speed using an error signal (difference between actual speed and target speed).
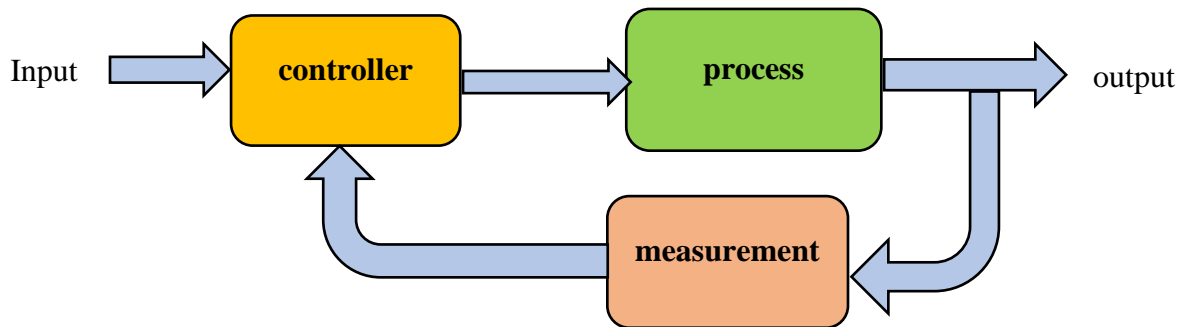

Fig 1) Block diagram of a closed loop control system

Closed loop control in neuroscience

For decades, the brain has been treated as a block box in open loop approaches by imposing a pre-defined stimulus (usually sensory stimulation) in a controlled laboratory environment and exploring the input and output relationship and how they are modulated (Figure 1). However, many

functions in the nervous system are actually implemented in a closed loop manner. Also the nervous system itself is embedded in a closed loop system; sensory input changes depending on the behavior (i.e. motor output) of the organism. The brain operates as a generator of behavior which continuously interacts with its surrounding environment. In fact, behaving animal can influence the environment which can change the sensory input. Therefore, it is important to gain better understanding of the nervous system in a closed loop manner instead of a traditional open loop approach.
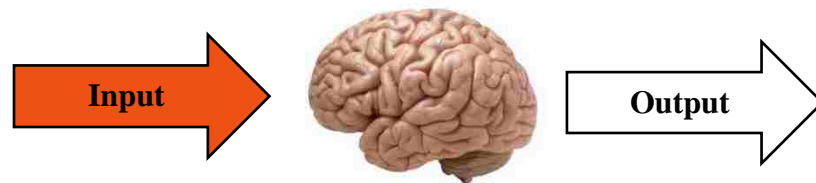
Open-Loop

Fig 2) A typical open loop experiment in neuroscience. Input is usually delivered via sensory organs. Output is sometimes measured in terms of neural response to input, but ultimately, the output of the brain are the signals which control muscles and generate behavior.

In neuroscience, closed loop control systems refer to two conceptually different categories of loops. In ongoing brain activity dynamics loop, the fluctuation of neural activity (output) influences and changes the evoked stimuli (input). In this case, however, environmental dynamics are assumed to be stateless and static, therefore, stimuli don't get any direct influence from outside of the brain

A more complicated closed loop scenario, behavior-in-the-loop, acknowledges that the environment retains its own dynamical state comprising of the equation of motion ruled by laws

of physics and observable state. Therefore, the stimuli influencing the ongoing brain activity changes by the interaction of motor and sensory systems. In other words, a task dynamic loop deals with the active interaction of brain and real-world environment or computer simulated environment to maintain a goal oriented behavioral task.

The most comprehensive and efficient close loop neuroscience is the combination of ongoing brain activity triggered and behavior in the loop which controls the internal brain activity of the animal while performing a behavioral task.

Closed-Loop system in physiology

Implementing the closed loop control system with a time scale of millisecond allows selective manipulation of the internal state of the brain that can lead to answering many open questions in neurophysiology. Such as which oscillation frequencies occur during specific behaviors? How does noninvasive brain stimulation, like transcranial magnetic stimulation, induce activity in spinal cord and cortex?

In a recent study, scientist carried out a closed loop control system and trained monkey to move a cursor toward a target, causing the enhancement of the low-gamma frequency power in a specific site of the motor cortex. They showed that high power of low gamma frequency of LFP in monkey was accompanied with the synchronized ongoing brain activity. Volitional manipulation of ongoing internal firing pattern offers a promising and unique approach for neural processing [27].

In another study, investigators implemented a closed loop control system in a freely moving rabbit performing memory and learning. They monitored the pre-existing state of the hippocampus just before the task. They classified the pre-existing state into two categories of low LFP frequency

(theta oscillation 2-8Hz) and high LFP frequency (non-theta 8-22 Hz), they found a strong correlation between pre-existing ongoing patterns and learning task, in fact, the rabbit learned at a faster rate in theta frequency than non-theta frequency. These types of research can help to better understand the neural processing and mechanism of learning and memory. Also, these results suggest that there might exist an optimal state that animal performs the best and most efficient functionality.

In another important example of closed loop related to memory, the closed loop simulation was implemented to stimulate the auditory system during <1 Hz slow-wave sleep in sleeping humans. Such slow wave oscillation plays an important role in consolidation of memory during sleep. It was shown that closed loop stimulation during slow oscillation up states enhanced the slow oscillation and, in turn, enhanced memory consolidation while stimulation out phase with ongoing rhythmic remained ineffective [28].

Nonetheless, designing an experiment with a well-controlled physical environment for an awake behaving animal, and quantifying the motor and sensory interplay, can be very challenging. Therefore many studies have recently done with a 'virtual reality', computer simulated environment[29],[30],[31],[32].

Closed loop system in neurological therapy

Closed loop systems have great potential for treatment of neurological disorders caused by network dysregulation. In neurological therapy, closed loop system used to either re-set the local excitability and neural activity or induce plasticity to re-wire connectivity damaged due to neurological disorders.

For example, in a recent study, deep brain stimulation feedback control was carried out to treat the Parkinson disease by delivering the adaptive deep brain stimulation when beta oscillation power in LFP exceeded a threshold. Closed loop approaches were more efficient, with fewer side effects and cost compared to open loop deep brain stimulation[33],[34].

Optogenetic stimulation

Optogenetics is a technique that enables targeted control over the specific well-defined events in neural circuits. This new technology allows the high temporal precision control of specific neurons to better understand the underlying mechanism of circuit function.

In optogenetic techniques, neurons are genetically modified to express a light-activated protein called opsin. Depending on what type of opsin has been expressed in neurons, they will be activated or inhibited or detect neuronal activity when exposed to a specific frequency of light. Optogenetic techniques has recently improved extensively and offers a variety of opsins with a range of timescales to control neural activity [35].

Microbial opsins

Microbial opsins, found in a microorganism called algae, are light sensitive proteins that can induce or suppress the action potential when exposed to the specific frequency of light. Channelrhodopsin2 (Chr2) is a blue light sensitive light protein that opens non-specific cation channels in the neuron membrane, causing the neuron to depolarize and fire one or more action potentials. Halorhodopsins (HR) is a green/yellow light sensitive protein that pumps chloride ions out of the neuron, causing depolarization of the membrane potential, which inhibits action potentials. Archaerhodopsin (Arch) works the same as Halorhodopsins (HR) except pumping out hydrogen ions instead of chloride ions.

Closed-loop optogenetic

Closed-loop optogenetic allows a neuroscientist to deliver optical stimulation or inhibition based on currently observed neural activity. Input in a closed loop optogenetic system is a tunable light stimulus which is regulated based on an error signal (the difference between target and measured output).

Although many optogenetic experiments have been implemented to guide the neural activity, most of them can be categorized as open loop optogenetic control or activity-guided control thus not many closed loop optogenetic control have accomplished by neuroscientists so far. Indeed, observed neural activity was used to select the stimulus parameters based on earlier published neural activity recording [37], [38], [39]. But this was done without feeding back the outcome of stimulation on neural activity to modulate the optical stimulation parameters in real time. In

contrast, online readout of recording neural activity such as electrophysiological or behavioral data is processed to modulate optical stimulation or inhibition parameters (frequency, intensity, etc.) in the closed loop optogenetic.

For example in a recent study, optogenetic techniques were implemented to demonstrate that firing pattern in pyramidal cells modulates gamma frequency in local field potential, furthermore, it was shown that increasing gamma frequency power enhanced the information processing [40]. While open loop stimulation also could induce the gamma frequency, closed loop inhibition of spikes illustrated a cause and effect relation between increasing gamma frequency power and enhancement of information flow which couldn't be achieved by open loop inhibition approaches[32].

Light illumination in optogenetic

Light sources are a key part of experimental set-up in optogenetic control, Lasers and LEDs are two popular light sources in optogenetic for illuminating the light sensitive opsins. Either of laser of LED can be used depending on experiment. Lasers supply a narrow bandwidth of light with efficient coupling to fiber optics. High power and narrow bandwidth frequency of lasers permits the deep brain stimulation or inhibition of single neurons in transgenic animals. While LEDs are useful because of their low cost and diverse choice of wavelengths. Small size and low power of LEDs make them an ideal choice for multisite photo stimulation and portable devices.

Optogenetic drawbacks

Recent development in optogenetic enables neuroscientist to manipulate the selected neurons activity within complex neural network with high level of precision. It permits researchers to disclose how neural circuit activities regulates the behavior, however they have some drawbacks in terms of applications and efficiency. For example, optogenetic stimulation might causes some abnormal unintended physiological activities with unpleasant consequences. In many photo-excitation and photo-inhibition, firing rates evoked are at the extreme end of naturally occurring spontaneous firing activity, therefore they could push firing rates outside of normal physiological ranges.

Also, pulsed optogenetic stimulation can induce intense synchrony and correlation among large populations of stimulated or inhibited neurons, since frequency and synchrony are the main foci of many researchers that study physiological recordings during behavior, induced frequencies can be confusing and troublesome. Furthermore, illuminating the neural tissue is spatially non-uniform causing different level of activities throughout the illuminated area. Finally, optogenetic techniques manipulate the electrical activity of all targeted population of neurons and can't easily target subset of neurons.

Experimental preparation

All animal procedures were in accordance with guidelines of Care and Use of Laboratory Animals of the National Institutes of Health and approved by University of Arkansas Institutional Animal Care and Use Committee under Animal Use Protocol 17003.

Genetically modified female mice were used (19█2 gr, Genotype: Homozygous for Tg(Thy1-COP4/EYFP) 18Gfng, Jackson laboratory, ME, USA). Thy1-ChR2-YFP transgenic mice express Channelrhodopsin-2, which functions as a light-activated ion channel.

Channelrhodopsin-2 from the green alga Chlamydomonas reinhardtii are one of the first discovered Channelrhodopsin-2. They bind to Yellow Fluorescent Protein (ChR2-YFP) under the control of the mouse thymus cell antigen 1 (Thy1) promoter. The ChR2-YFP protein is expressed in all neurons throughout cortex, hippocampus, thalamus, midbrain, and brainstem. Morphological and physiological properties of transgenic neuron is fairly similar to counterpart intact neurons [35].

The mice were anesthetized using vaporized isoflurane. Initial induction of anesthesia was done by placing the mouse in a closed box, through which a mixture of oxygen and isoflurane was flowing. Anesthesia was maintained throughout the rest of the experiment using an Isoflurane Low-Flow Anesthesia Systems (SomnoSuite, Kent Scientific Corporation). The anesthetic was mixed with medical-grade carbogene (95% oxygen and 5% carbon dioxide) and delivered directly to the animal through a mask that fit tightly over the mouse's snout. This allowed us to maintain a stable and accurate level of anesthesia. Using the SomnoSuite, isoflurane concentration was tunes

The mice were mounted in a stereotaxic frame and head-fixed with two ear bars. A 3 mm $\times$ 3 mm craniotomy (1 mm posterior from bregma, 3 mm lateral from midline) was performed over the motor cortex to allow access to the motor cortex of the mouse (Figure 3).
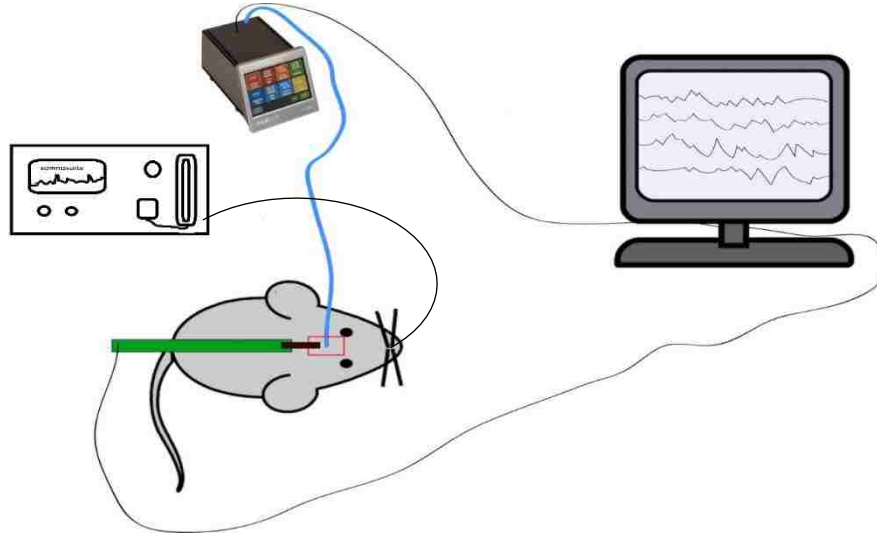
Fig 3) A cartoon illustration of experimental setup.

Multielectrode recording

Multielectrode recording were obtained from motor cortex, using 32-channel microelectrode arrays (8 shanks, 4 electrodes, [B8D3], Neuronexus, MI, USA). Electrode signals were digitalized and sampled at 30 kHz using Blackrock microsystem (Cereplex + Cerebus, Blackrock Microsystems, UT, USA). After inserting the electrodes to a depth of 650 microns, the craniotomy was covered with small gel foam pieces, soaked in saline. Voltages were referenced to Ag-AgCl pellet placed in the gel foam pieces.

Local field potential

The brain signals we used in our closed-loop feedback system were mid- to high-frequency local field potentials. Voltages were first band pass filtered between 10 and 250Hz. Then negative peaks in the LFP fluctuations were detected by thresholding at -30 μv. The rate of these LFP peak

42

events, hereafter referred to as 'activity rate', was the variable that we controlled in our experiments. The LFP peaks were detected using the Cerebus system. This data was directly accessed, in real time, by Matlab for use in closed-loop feedback control as described more below.

Data Analysis

All data analysis was performed in MATLAB (Mathworks). As discussed further below, the Controllability of the neural network was defined as the SAE(sum of the absolute values) of differences between the target activity rate time series and the measured firing rate time series. 'Energy' needed to maintain the target activity rate were defined as the integral of the LED control voltage time series during the control period. Correlation coefficients between Controllability and Energy were computed using the function

$$corr(x, y) = \frac{cov(x, y)}{\sigma_x \sigma_y}$$

Where cov is covariance and σ is standard deviation.

Optical stimulation

A 470 nm LED was coupled to a 125 µm optical fiber using the butt-coupling technique. To minimize the losses at the fiber input and maximize the output power, the fiber connector was placed in a way that the end of fiber was as close as possible to the emitter. The other end of the fiber optic was positioned so that its tip was in contact with the brain surface approximately 1 mm away from the insertion point for the microelectrode array. The fiber optic was fixed in place

43

using a micromanipulator. An implantable fiber optic cannula was used to decrease the numerical

aperture to (NA) 0.39. The micromanipulator was attached to stereotactic frame.

Optical stimulation protocol

The LED driver mode was set to 'external modulation' and was controlled by Matlab Online

interface (CBMEX) output. Matlab was used to control an analog output of the Blackrock Cerebus

system, which was connected the LED driver. Each recording trial last for 300sec. During the

first 180 sec, the LED control voltage was set to zero (no light output), during which we recorded

spontaneous neural activity. During the next 30 sec, closed-loop optical stimulation was used to

attempt to control the activity rate of the motor cortex. The activity rate was measured and the

LED control voltage was updated every 15 ms. Finally the LED voltage was set back to zero to

record the post stimulation effects.

Average firing rate

The feedback controller was carried out using a toolkit of Matlab functions provided by Blackrock

which allowed access to the data in real time as it was being recorded. Matlab was used to count

the total number of negative LFP peaks recorded from all 32 electrodes every 15 ms. Since this

count was often zero, we temporally smoothed the activity rate of network using a first-order

averaging filter as done in previous studies [32].

$$\bar{r}(k) = \alpha r(k) + (1 - \alpha)\bar{r}(k - dk) \tag{1}$$

Where $r(t) = \frac{number\ of\ spikes}{\Delta t}$ represents the instantaneous firing rate with $\Delta t = 15ms$

A is weighting factor, choosing appropriate value for α was crucial and changed the quality of control significantly,

. A small enough value of α resulted in an excellent control, but in expense of smoothing out the average firing rate, and large value of alpha resulted in the high fluctuation of average firing rate which was very difficult to control. To set the best value for α , a range of values between $0.0001 < \alpha < 0.1$ was tried and $\alpha = 0.01$ found to be the smallest value that lead to reasonable control.

Proportional controller

Matlab was used to implement a proportional feedback controller with the goal of controlling the neural activity to a desired rate of LFP peaks. The averaging firing rate was subtracted from a target firing rate ▮ to calculate the error.

$$e = \bar{r}^* - \bar{r}(t) \tag{3}$$

This value was used to update the voltage of the LED in real time (15 ms temporal resolution). starting from an initial voltage before control set to zero. Voltage was measured in mV

$$V = V + P * e \tag{4}$$

Parametric sensitivity of controller, was chosen by trying out different values of P, while keeping other parameters fixed.   any value in the range of (0.01<P<0.5) did not change the control significantly, therefore P=0.1 was used throughout the following experiments for consistency.

Target firing rate

Due to high variability from animal to animal, spontaneous activity rate varied a lot from experiment to experiment. Therefore, two different methods of choosing a target rate were tried. The first method was to settle target rate based on the rate of ongoing activity recorded during the 5 minutes prior to starting control. Target rate was set to 4, 5 or 8 times of average spontaneous activity rate. The second method was simply to set the target rate to 25, 50 or 70 irrespective of the ongoing activity rate.

Results

Hypothesis

Here we implement a closed loop feedback control to induce and maintain a specific neural activity rate in motor cortex. First, we hypothesized that our ability to control the activity rate will depend on the cortical state of the animal. More specifically, we hypothesized that there exists a state-dependent trade-off between the accuracy of control and the cost to maintain control. That is, some cortical states may allow very accurate control, but require excessive control 'energy', while other cortical states require less energy, but are more prone to control errors. Thus, we hypothesize that an optimal cortical state can be found that compromises between accuracy and cost. We first

46

developed the hypothesis based on a study using a computational model and then we experimentally confirmed the hypothesis.

Model results

We developed a network level computational model consisted of 2000 binary neurons with 80% excitatory and 20% inhibitory neurons. To model changes in cortical state, we manipulated inhibitory synapses, which resulted in dramatic changes in the ongoing dynamics of the neuronal population. By tuning the inhibitory synapses, various dynamic states ranging from low to high rate spiking activity was generated (Fig 4-6a).

A proportional feedback controller was used to control the model neural spike rate. A target spike rate was maintained by a feedback closed loop approach. The difference between current spiking rate and targeted spike rate was used as an error signal to change the input to the model neurons. Feedback control was maintained during 60 time model time steps after a period of 180 time steps pre stimulation without control and before a period of 60 time step post stimulation without control (Fig 4-6 b,c).

We quantified the control based on two factors: 1) how accurate the spiking rate can be fixed at a constant target rate level as

$$Error = \sum_{t=1}^{60} |spike\ rate\ (t) - target\ rate|$$

and 2) how much 'energy' is required to maintain the targeted spiking activity as

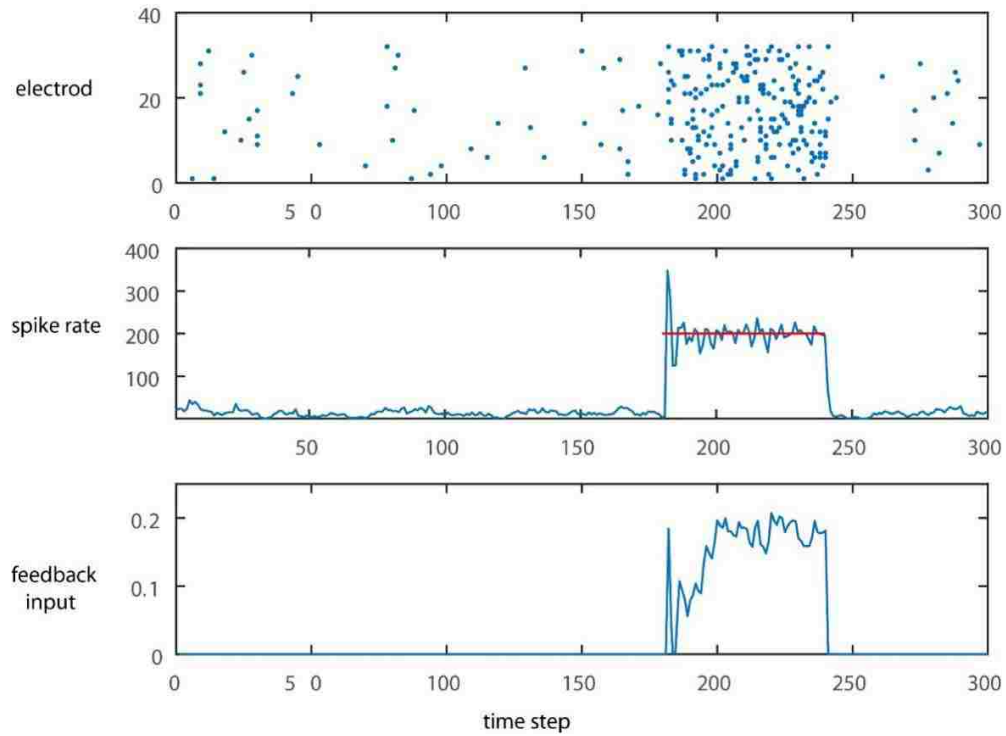$$Energy = \sum_{t=1}^{60} P \times |spike\ rate(t) - target\ rate|$$

Fig 4) Feedback control of firing rate: enhanced inhibition. Feedback control of firing activity over 60-time step for enhanced inhibition of synaptic weight a) Spike raster plot b) Averaged spike rate c) feedback control signal input into the network.
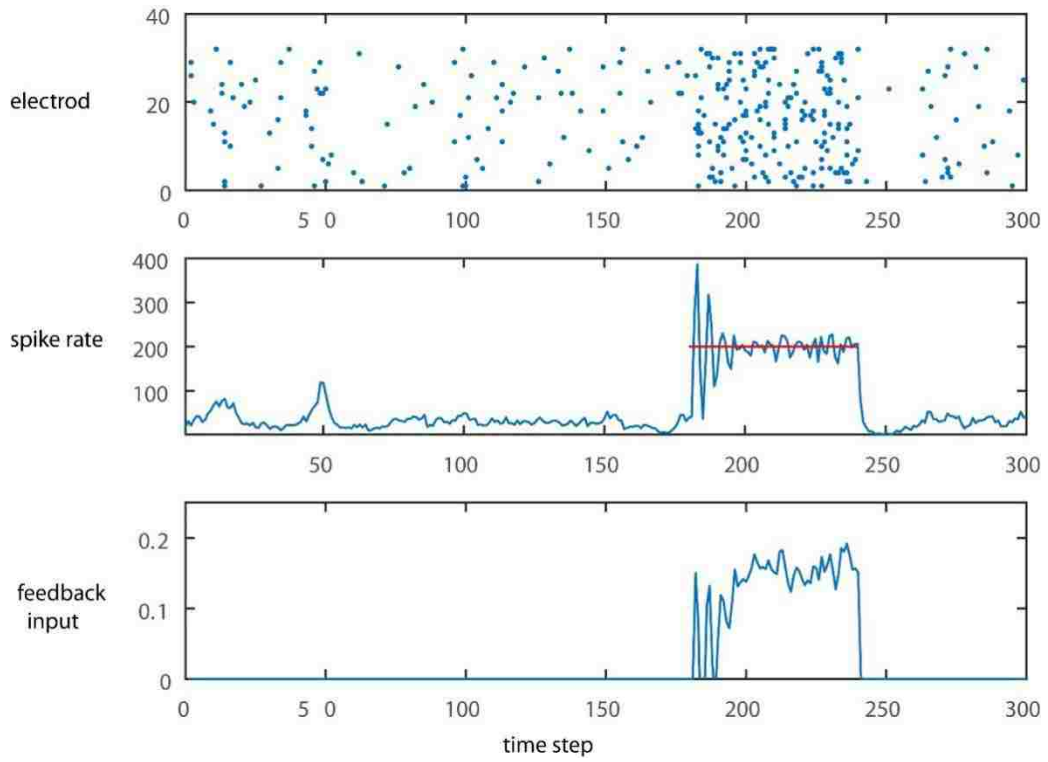
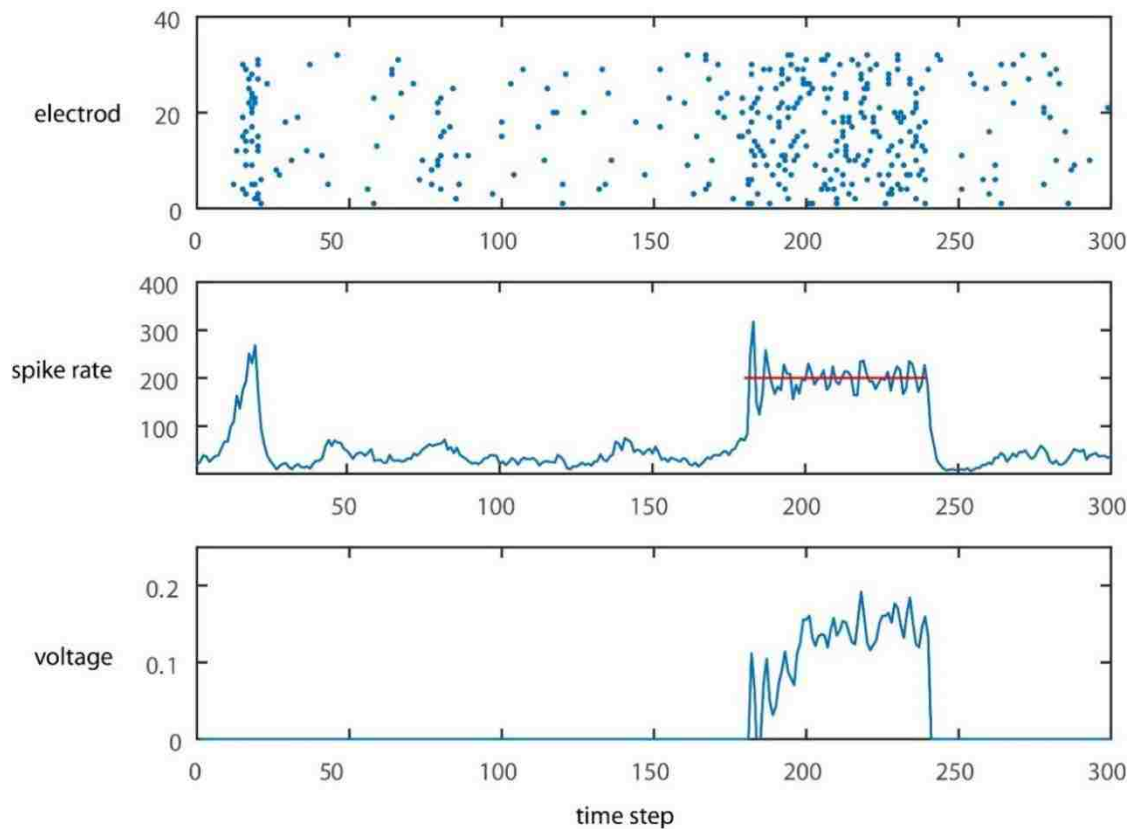Figure 5) Feedback control of firing rate: balanced inhibition

Fig 6) Feedback control of firing rate: reduced inhibition

The controllability of the network changed significantly as the dynamic state shifted the low firing state (Fig 4) to the high firing state (Fig 6). Low spiking rate dynamic activity required the highest energy but it maintained the most accurate control, while the high spiking rate dynamic required the lowest energy, but had the lowest accuracy (Fig 7). Therefore, we predicted a trade-off between accuracy of the control and energy required to maintain the control. Decreased control energy in the high firing state makes sense since less external input was required to increases the spiking activity to reach the target rate. However increasing the accuracy by decreasing the population activity was less obvious.
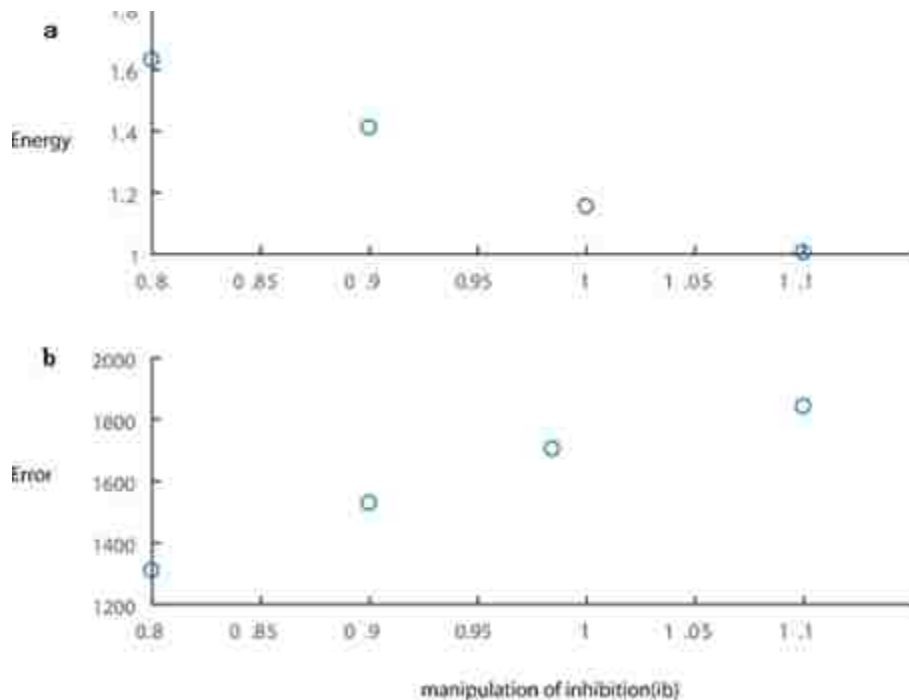
50

Fig 7). Energy and error trade off. Here each point represents one control trial from the model. Inhibition is decreased from left to right along the horizontal axis. a) Energy required to control the firing rate at the neural network decreases as inhibition was decreased. b) Error between the targeted firing rate and measured firing rate increases as inhibition decreases. These results suggest that an intermediate level of inhibition is required to balance between low energy consumption and low control error.

Experimental results

We tested the trade-off hypothesis in experiments by implementing a closed-loop optogenetic feedback control neural activity in mouse motor cortex. In our model, we obtained a continuum of dynamical states by varying synaptic inhibition. Similarly, in our experiments, we obtained a continuum of cortical states by varying the level of isoflurane anesthesia, which also is known to affect inhibitory synapses. If our experiments agree with our model predictions, we expect to find that control error is inversely related to the control energy.

51

We recorded local field potential (LFP) in motor cortex of anesthetized transgenic female mice using 32-channel micro-electrode arrays. Recordings were filtered between 10 and 250 Hz and thresholded at -30 µv to detect high frequency LFP peaks. The average activity rate over all electrodes was estimated and temporally smoothed using a first-order averaging filter (more details in material and method section). A 470 nm LED was coupled to a 125 µm optical fiber to optogenetically stimulate the motor cortex of the mouse. The control voltage of the stimulation LED changed based on difference between the estimated spiking rate and a targeted spike rate. Similar to model, each experimental trial was broken up into three periods: 60 second of feedback control after a 240 second pre-stimulation period and before a 60 seconds post stimulation period (Fig 8-10). As shown in previous studies[41] we observed that as isoflurane was increased, and the animals were more deeply anesthetized, firing rate decreased and the neural activity was more similar to enhanced inhibition firing activity of our model.
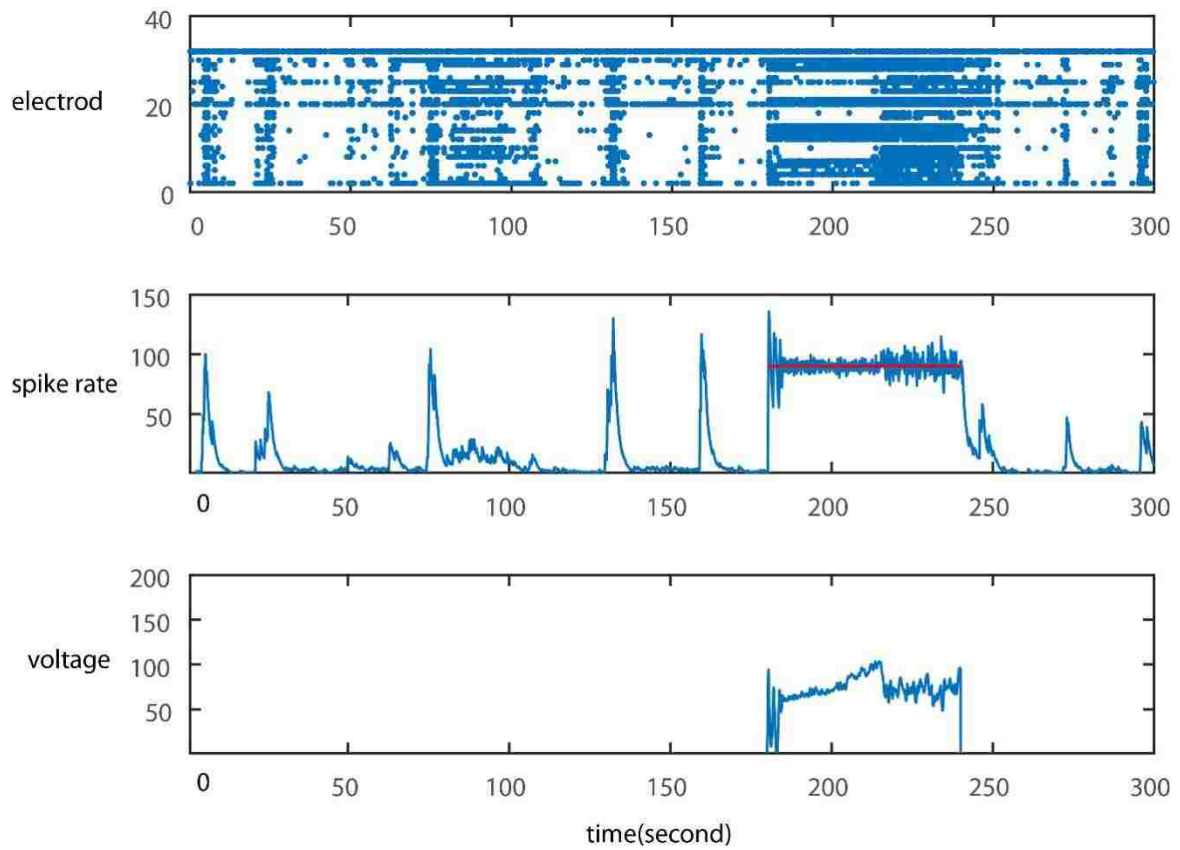
Fig 8) Closed loop feedback control of neural activity for a low flow rate isoflurane(high firing activity) case. a) LFP peak activity raster plot b) activity rate c) LED control voltage.
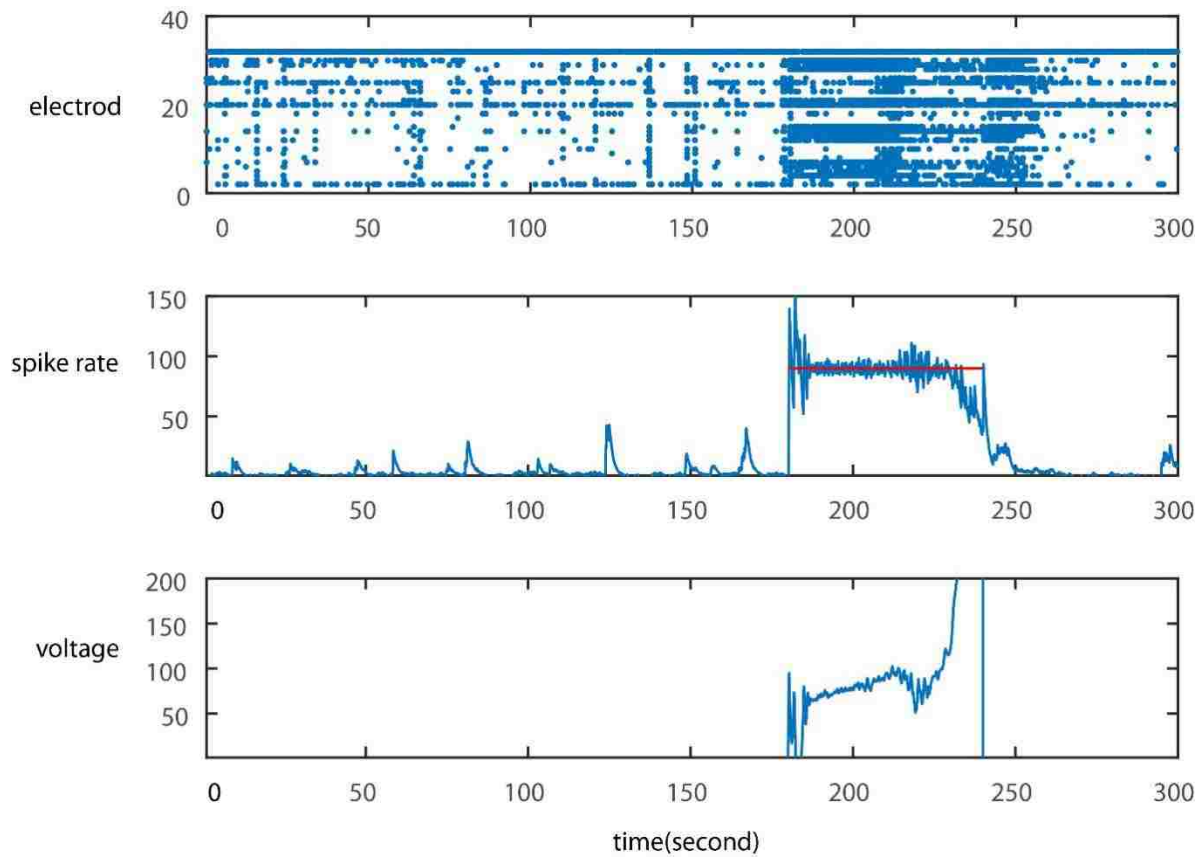
Fig 9) The same as Fig 5 except for a case of medium isoflurane flow rate (medium firing activity)
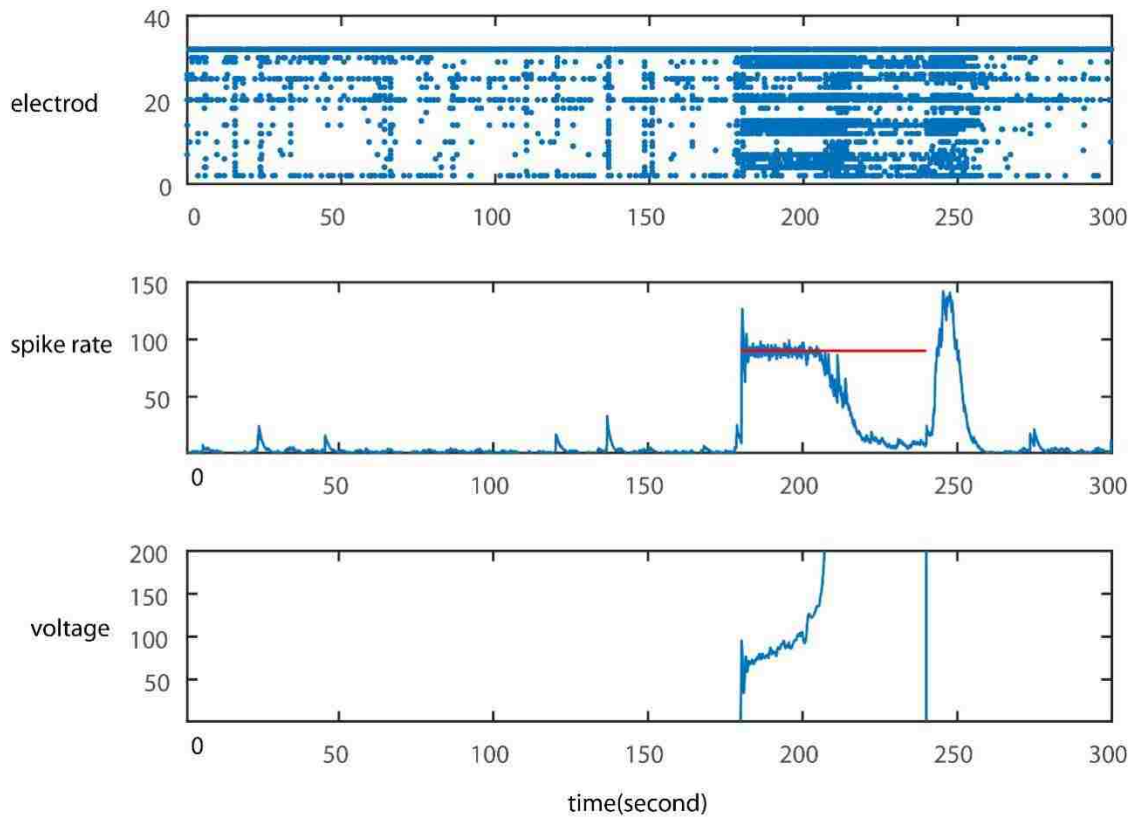
Fig 10) The same as Fig 5 except for a case of high isoflurane flow rate (low firing activity)

Evaluating the Hypothesis

We carried out the closed loop feedback on various ongoing activity ranging from low to high rate firing activity. We are still working on this project, but the primary results we found were very interesting and promising. We measured a significant anti-correlation between energy and accuracy of controlling the neural firing activity as it was predicted earlier by the model. Quantitatively, we found a Pearson correlation coefficient < -0.9 and significance<0.05 (example results from three different mice with their correlation are shown in (Fig 8-10). Thus the most accurate control comes at the cost of consuming higher energy, however despite the model

prediction, energy and error didn't correlate with the anesthetic level (Fig 8-10). This may be because the effects of anesthesia vary from animal to animal and from hour to hour within one animal. One way that we hope to deal with this issue is to develop a better way to assess the cortical state that is more reliable than the isoflurane concentration. We hope to analyze the recording of ongoing activity prior to control to get a more precise quantitative measure of the cortical state that is insensitive to the nonstationary changes in depth of anesthesia that are very difficult to control experimentally.

Fig 11) An example of strong anticorrelation between the energy and error (pairwise linear correlation ρ=-0.9833 and significant P=0.0167). a) Energy. b) Error
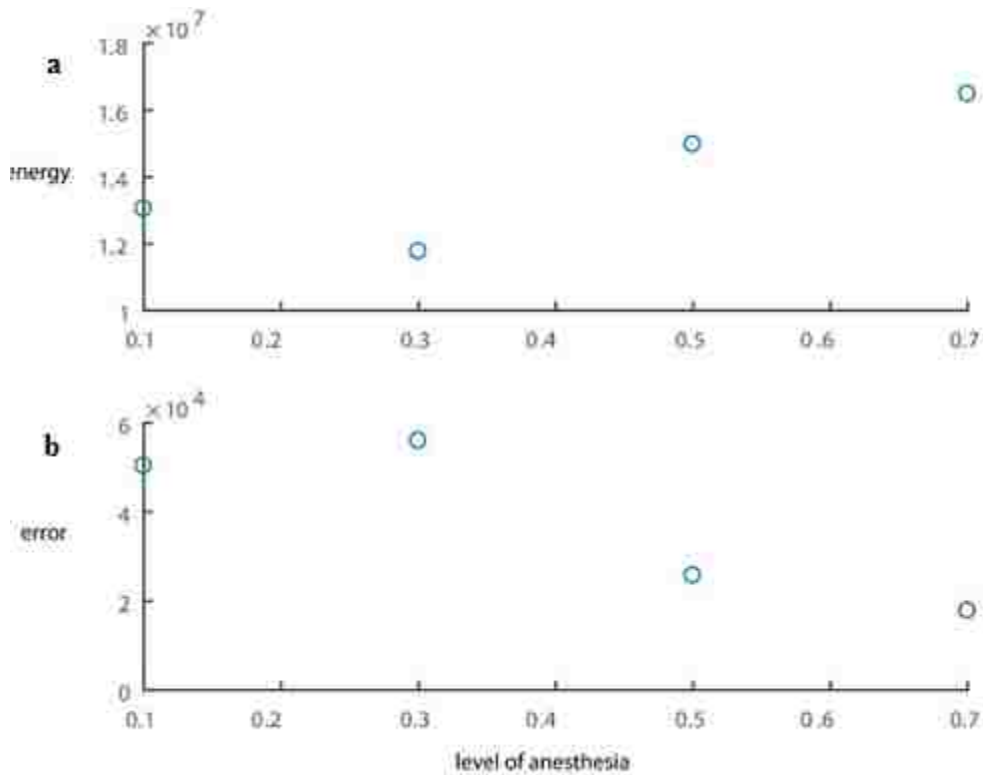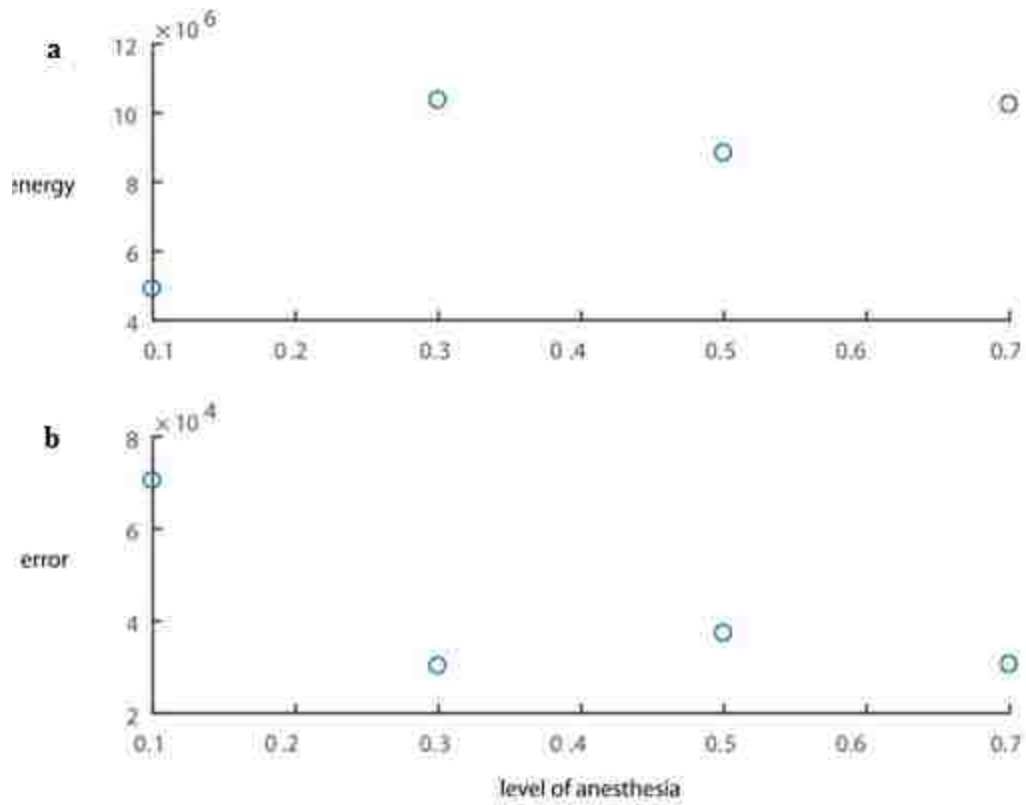
Fig 12) An example of strong anticorrelation between the energy and error (pairwise linear correlation ρ=- 0.9946 and significant P=0.0054). a) Energy b) Error
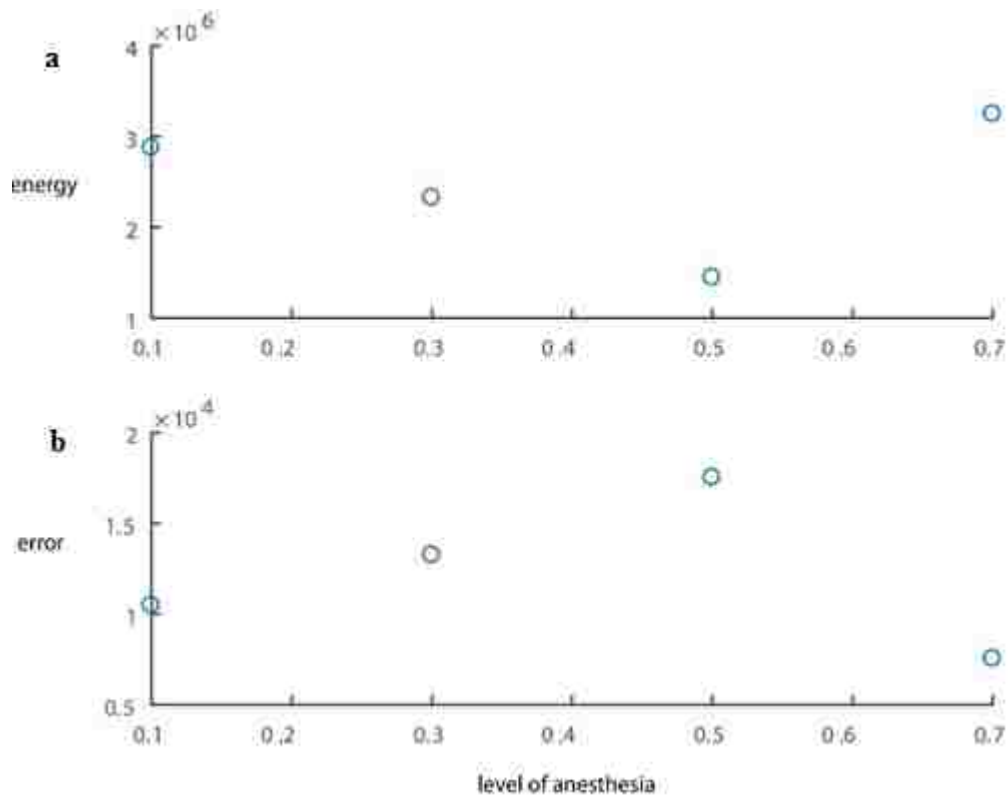
Fig 13) An example of strong anticorrelation between the energy and error (pairwise linear correlation ρ=- 0.9951 and significant P=0.0049). a) Energy b) Error

Rebound effect

We observed an interesting effect in the experiment which didn't match the model prediction whenever cortex adapted to the light. In that case immediately after stopping the LED light cortex started a significant firing activity. This effect was consistent through all experiment (5 mice and trails). Few examples are shown in Fig 14. Further experiments are required to better understand this adaptation-rebound effect.
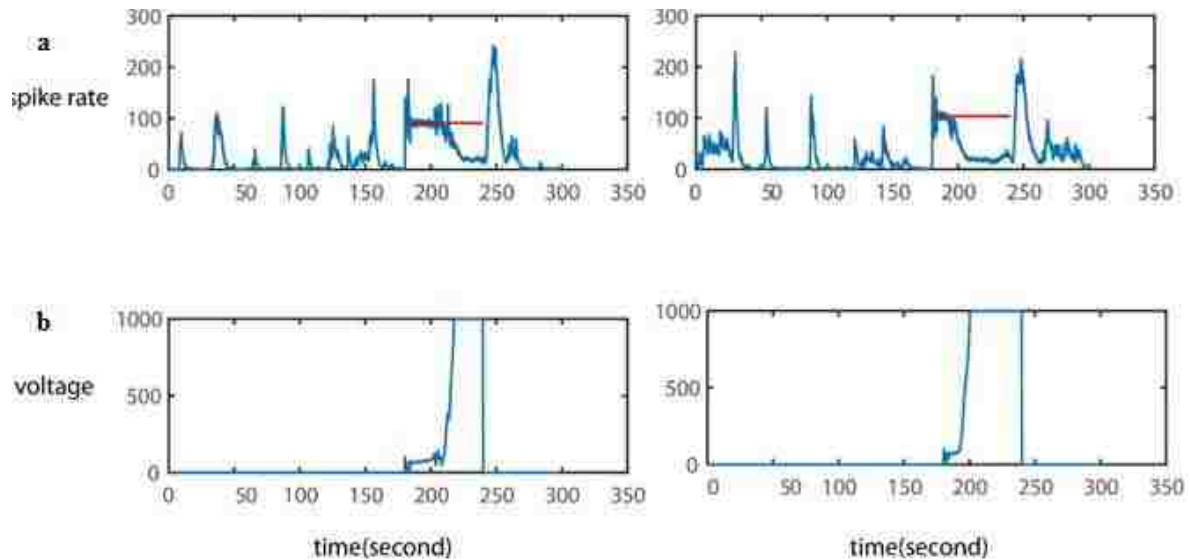
Fig 14) Significant firing activity following adaptation. a) Spiking activity. b) LED voltage.

Conclusion

In conclusion, we carried out a closed loop feed back control system to lock the firing activity of motor cortex of isoflurane anesthetized mice at a targeted firing rate. We found controllability changes as spontaneous neural activity varies. We found a trade off between the accuracy of fixing the firing rate at target and energy needed to maintain the control, so that as neural states tuned from high firing rate pattern to low firing pattern error decreased while the energy increased.

References

1.   Tolhurst, D.J., J.A. Movshon, and A.F. Dean, *The statistical reliability of signals in single neurons in cat and monkey visual cortex.* Vision Res, 1983. **23**(8): p. 775-85.

2.   Tsodyks, M., et al., *Linking spontaneous activity of single cortical neurons and the underlying functional architecture.* Science, 1999. **286**(5446): p. 1943-6.

3.   Nauhaus, I., et al., *Stimulus contrast modulates functional connectivity in visual cortex.* Nat Neurosci, 2009. **12**(1): p. 70-6.

4.   Chen, Y., W.S. Geisler, and E. Seidemann, *Optimal decoding of correlated neural population responses in the primate visual cortex.* Nat Neurosci, 2006. **9**(11): p. 1412-20.

5.   Arieli, A., et al., *Coherent spatiotemporal patterns of ongoing activity revealed by real-time optical imaging coupled with single-unit recording in the cat visual cortex.* J Neurophysiol, 1995. **73**(5): p. 2072-93.

6.   Sporns, O. and R. Kötter, *Motifs in brain networks.* PLoS Biol, 2004. **2**(11): p. e369.

7.   Arieli, A., et al., *Dynamics of ongoing activity: explanation of the large variability in evoked cortical responses.* Science, 1996. **273**(5283): p. 1868-71.

8.   MacLean, J.N., et al., *Internal dynamics determine the cortical response to thalamic stimulation.* Neuron, 2005. **48**(5): p. 811-23.

9.   Cossart, R., D. Aronov, and R. Yuste, *Attractor dynamics of network UP states in the neocortex.* Nature, 2003. **423**(6937): p. 283-8.

10.   Ikegaya, Y., et al., *Synfire chains and cortical songs: temporal modules of cortical activity.* Science, 2004. **304**(5670): p. 559-64.

11.   Buzsáki, G., C.A. Anastassiou, and C. Koch, *The origin of extracellular fields and currents--EEG, ECoG, LFP and spikes.* Nat Rev Neurosci, 2012. **13**(6): p. 407-20.

12.   Harris, K.D. and A. Thiele, *Cortical state and attention.* Nat Rev Neurosci, 2011. **12**(9): p. 509-23.

13. Clement, E.A., et al., *Cyclic and sleep-like spontaneous alternations of brain state under urethane anaesthesia.* PLoS One, 2008. **3**(4): p. e2004.

14. Greenberg, D.S., A.R. Houweling, and J.N. Kerr, *Population imaging of ongoing neuronal activity in the visual cortex of awake rats.* Nat Neurosci, 2008. **11**(7): p. 749-51.

15. Crochet, S. and C.C. Petersen, *Correlating whisker behavior with membrane potential in barrel cortex of awake mice.* Nat Neurosci, 2006. **9**(5): p. 608-10.

16. Poulet, J.F. and C.C. Petersen, *Internal brain state regulates membrane potential synchrony in barrel cortex of behaving mice.* Nature, 2008. **454**(7206): p. 881-5.

17. Luczak, A., et al., *Sequential structure of neocortical spontaneous activity in vivo.* Proc Natl Acad Sci U S A, 2007. **104**(1): p. 347-52.

18. Luczak, A., P. Barthó, and K.D. Harris, *Spontaneous events outline the realm of possible sensory responses in neocortical populations.* Neuron, 2009. **62**(3): p. 413-25.

19. Sakata, S. and K.D. Harris, *Laminar structure of spontaneous and sensory-evoked population activity in auditory cortex.* Neuron, 2009. **64**(3): p. 404-18.

20. Okun, M., A. Naim, and I. Lampl, *The subthreshold relation between cortical local field potential and neuronal firing unveiled by intracellular recordings in awake rats.* J Neurosci, 2010. **30**(12): p. 4440-8.

21. Otazu, G.H., et al., *Engaging in an auditory task suppresses responses in auditory cortex.* Nat Neurosci, 2009. **12**(5): p. 646-54.

22. Atiani, S., et al., *Task difficulty and performance induce diverse adaptive patterns in gain and shape of primary auditory cortical receptive fields.* Neuron, 2009. **61**(3): p. 467-80.

23. Curto, C., et al., *A simple model of cortical dynamics explains variability and state dependence of sensory responses in urethane-anesthetized auditory cortex.* J Neurosci, 2009. **29**(34): p. 10600-12.

24. Hasenstaub, A., R.N. Sachdev, and D.A. McCormick, *State changes rapidly modulate cortical neuronal responsiveness.* J Neurosci, 2007. **27**(36): p. 9607-22.

25.   Deco, G., V.K. Jirsa, and A.R. McIntosh, *Emerging concepts for the dynamical organization of resting-state activity in the brain.* Nat Rev Neurosci, 2011. **12**(1): p. 43-56.

26.   Fox, M.D. and M.E. Raichle, *Spontaneous fluctuations in brain activity observed with functional magnetic resonance imaging.* Nat Rev Neurosci, 2007. **8**(9): p. 700-11.

27.   Engelhard, B., et al., *Inducing γ oscillations and precise spike synchrony by operant conditioning via brain-machine interface.* Neuron, 2013. **77**(2): p. 361-75.

28.   Ngo, H.V., et al., *Auditory closed-loop stimulation of the sleep slow oscillation enhances memory.* Neuron, 2013. **78**(3): p. 545-53.

29.   Shahaf, G. and S. Marom, *Learning in networks of cortical neurons.* J Neurosci, 2001. **21**(22): p. 8782-8.

30.   Chao, Z.C., D.J. Bakkum, and S.M. Potter, *Shaping embodied neural networks for adaptive goal-directed behavior.* PLoS Comput Biol, 2008. **4**(3): p. e1000042.

31.   Keren, H. and S. Marom, *Controlling neural network responsiveness: tradeoffs and constraints.* Front Neuroeng, 2014. **7**: p. 11.

32.   Newman, J.P., et al., *Optogenetic feedback control of neural activity.* Elife, 2015. **4**: p. e07192.

33.   Little, S. and P. Brown, *What brain signals are suitable for feedback control of deep brain stimulation in Parkinson's disease?* Ann N Y Acad Sci, 2012. **1265**: p. 9-24.

34.   Little, S., et al., *Adaptive deep brain stimulation in advanced Parkinson disease.* Ann Neurol, 2013. **74**(3): p. 449-57.

35.   Rein, M.L. and J.M. Deussing, *The optogenetic (r)evolution.* Mol Genet Genomics, 2012. **287**(2): p. 95-109.

36.   Lin, J.Y., *A user's guide to channelrhodopsin variants: features, limitations and future developments.* Exp Physiol, 2011. **96**(1): p. 19-25.

37.   Gunaydin, L.A., et al., *Natural neural projection dynamics underlying social behavior.* Cell, 2014. **157**(7): p. 1535-51.

38.   Tsai, H.C., et al., *Phasic firing in dopaminergic neurons is sufficient for behavioral conditioning.* Science, 2009. **324**(5930): p. 1080-4.

39.   Schultz, W., *Multiple dopamine functions at different time courses.* Annu Rev Neurosci, 2007. **30**: p. 259-88.

40.   Sohal, V.S., et al., *Parvalbumin neurons and gamma rhythms enhance cortical circuit performance.* Nature, 2009. **459**(7247): p. 698-702.

41.   Alkire, M.T., A.G. Hudetz, and G. Tononi, *Consciousness and anesthesia.* Science, 2008. **322**(5903): p. 876-80.

Chapter 3

Abstract

A large population of neurons in cerebral cortex can produce diverse types of collective dynamics ranging from highly synchronized to desynchronized. Such differences in cortical state are typically studied using collective signals that average over many neurons. Little is known about how individual neurons participate in the collective dynamics. Here we hypothesize that different neurons imbedded in the same network can differ substantially in how they participate with the greater population; they can be strongly or weakly coupled to the population. Each of these scenarios has its own potential functional benefits in the cortex. Weak population coupling might enhance information capacity while strong population coupling might enhance the robustness of information transmission. Therefore, different population coupling can be functionally important in the cortex. Motivated by recent experiments in our lab, here we study population coupling in a network-level computational model. We show that neurons with high and low population coupling can coexist, and population coupling changes as we tune the inhibition.

Introduction

Collective network activity and single neurons

A large population of neurons can generate various population patterns ranging from synchronous and regular to desynchronized and irregular population activity, but how do individual neurons embedded in neural network correlate with the average activity of the population? Are individual neighboring neurons synchronized with overall firing of the population or do they fire

independently? Are neurons strongly correlated with a synchronized population pattern or they are weakly correlated?

Population coupling measures the relationship between individual neurons and the larger population of neurons in the network. It measures how the firing activity of each neuron is related to the summed activity of all the other neurons within the network.

Studying the correlated activity of neurons and population is beneficial to understand underlying sensory information and computation in the cortex. For instance, a neuron that fires in perfect synchrony with the population may be beneficial for contributing to a more robust population-level signal. The idea is if some other neuron receives input from a large number of synchronized neurons, it is more likely to receive their signal with less chance of corruption due to noise. On the other hand, if all neurons fire together in synchrony, then the repertoire of different firing patterns they can produce is vastly reduced. More independent firing supports a more diverse set of firing patterns, i.e. a greater information capacity [1].

Given that both strong and weak population coupling have potential benefits, a network that can do both could be optimal. That is, here we hypothesize that some neurons in the population will have high population coupling, while others simultaneously have low population coupling. This hypothesis is also motivated by experimental measurements from our own lab (not yet published) and others [2]. Moreover, we hypothesize that population coupling can change depending on changes in cortical state. This is also supported by experimental measurement from our lab (not yet published).

Material and methods

Computational model

A simple spiking model, consisting of N = 1000 binary neurons was developed. The state of neuron j at time t is

$$S_j(t) = \begin{cases} 1 & \text{with probability } p_j(t) \\ 0 & \text{with probability } 1 - p_j(t) \end{cases} \tag{5}$$

Where $S_j(t) = 1$ represents spiking and $S_j(t) = 0$ represents not spiking state of the neuron.

The firing probability depends on the summed input to the neuron

$$p_i(t) = \sigma\left(r_i(t) \left[\eta + \sum_{j=1}^{N} W_{ij} s_j(t-1) \right] \right) \tag{6}$$

Where η is external input

$$spike\ rate = \sum_j S_j(t)$$

$$\sigma(x) = \begin{cases} 0 & x < 0 \\ 1 & x > 0 \\ x & 0 < x < 1 \end{cases} \tag{7}$$

Where summation represents the input from all firing neurons at time t-1 that were connected to neuron j .

$$r_i(t) = (1 + \alpha[\sum_{t-T_r}^{t-1} s_i(\tau)])^{-1} \tag{8}$$

$r_i(t)$ is an activity-dependent factor which decreases the probability of firing if neuron has fired recently (i.e. within a 100-time step time period before time t), and α is a factor used to control the influence of this history-dependent depression term (here α is set to 0.1),

Network connectivity and synaptic weight was modeled by an N×N matrix with entries W_{ij} representing the connection from neuron j to neuron i. 90% of connections set to zero (not all neurons are connected), 20% of columns were multiplied by minus 1 to represent the inhibitory neurons. All elements of matrix were divided by the maximum eigenvalue of the matrix to assure that the network dynamics neither explode nor dies out [3]. The manipulation of inhibition discussed below was done by multiplying all the negative entries of W by a constant ranging from -0.2 to 0.2 to represent enhanced or suppressed inhibition, respectively. This change in inhibition was made after normalizing W by its largest eigenvalue.

Population coupling

We measured the population coupling as it was introduced by other studies [2]

$$C_{pop,i} = \frac{1}{N_i} \sum_{t=1}^{\tau} f_i(t) P_i(t)$$

Where $f_i(t)$ represents the spike count of neuron i in time bins of duration 50 time steps, N is the total number of spikes fired by neuron i over the entire duration τ=50000 time steps, and $P_i(t)$ is called population spike count time series defined as

$$P_i(t) = \sum_{j \neq i} f_j(t) - \mu_j$$

Where μ_j is average spike count of neuron j. Note that $P_i(t)$ excludes the spikes of neuron i. Thus, C_{pop} is similar to a correlation coefficient between the spike time series of one neuron and the population average.

Results

We developed a simple binary model to generate the firing rate of each cell and distribution of population coupling. We studied the correlated activity between neurons and population rate and how changing the balance between inhibition and excitation could affect the population coupling among neurons.

We built a network level computational model consisting of 1000 binary neurons with 80% excitatory and 20% inhibitory neurons (more details in material and methods). Population coupling was computed based on groups of 20 neurons

As it was shown experimentally in previous studies, we found that some neurons had a strong correlation with population rate while some others were weakly correlated [4]. We manipulated two aspects of the model to obtain various dynamical state of the neuronal population. We changed either the strength of inhibitory connections in the network or we changed the strength of external input. Both of these changes are motivated by experiments in which inhibition is altered with drugs that affect all inhibitory neurons throughout the nervous system. The idea is that changing inhibition globally, like in these experiments, can cause changes due to local changes in inhibition or due to inhibition among more distant neurons that changes the input to the local neurons being measured.

First we increased the local inhibition and while keeping external input fixed measured the firing rate and population coupling. We observed that both firing rate and population coupling decreased as inhibition increased locally (Figure 2). Second we fixed the inhibition and decreased the external

68

input (when inhibition act globally, increasing the inhibition may decrease the firing rate not only in the cortex but firing rate caused by external input such as thalamus)(Figure 3). We found out that decreasing the external input increased the population coupling significantly while changing firing rate slightly. This observation was more similar to what has been seen in experiments from our lab (not yet published).

Finally, since both these effects are likely to be present together in experiments, we combined changes inhibition and external input. We found that a combination of increased local inhibition and decreased external input can result in a net increase in population coupling, suggesting that the changes in input can be the dominant effect(Figure 4).
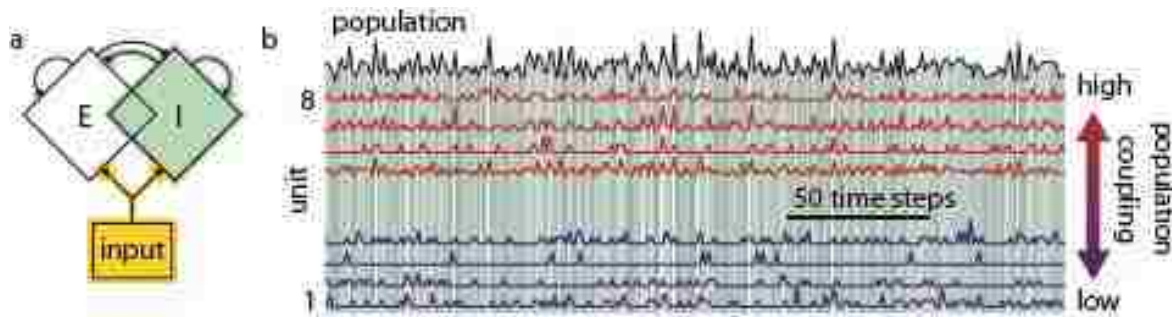

Fig 1) Neurons maintain high and low population coupling with population activity. a) Schematic of excitatory(E) and inhibitory(I) model of neurons with external input. Manipulating the inhibition globally, changes local inhibition(green) and external input(yellow) in the network. b) Examples of spike count time series with strong(red) and weak(blue) population coupling. Population rate is shown with black line and grayscale background
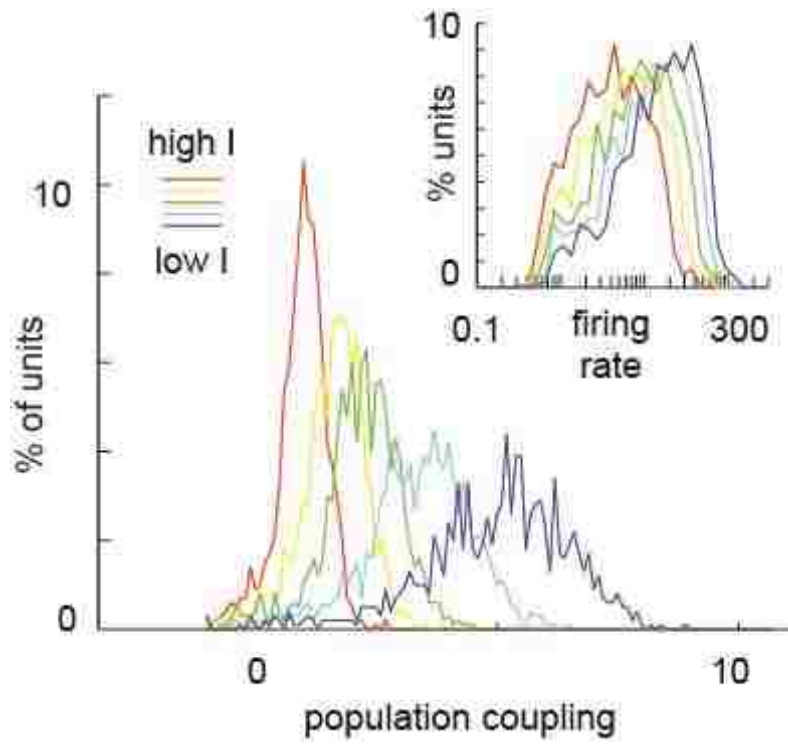
Fig 2) Tuning local inhibition alters the population coupling. Population coupling and firing rate(inset) increases as inhibition decreases (external input is constant)
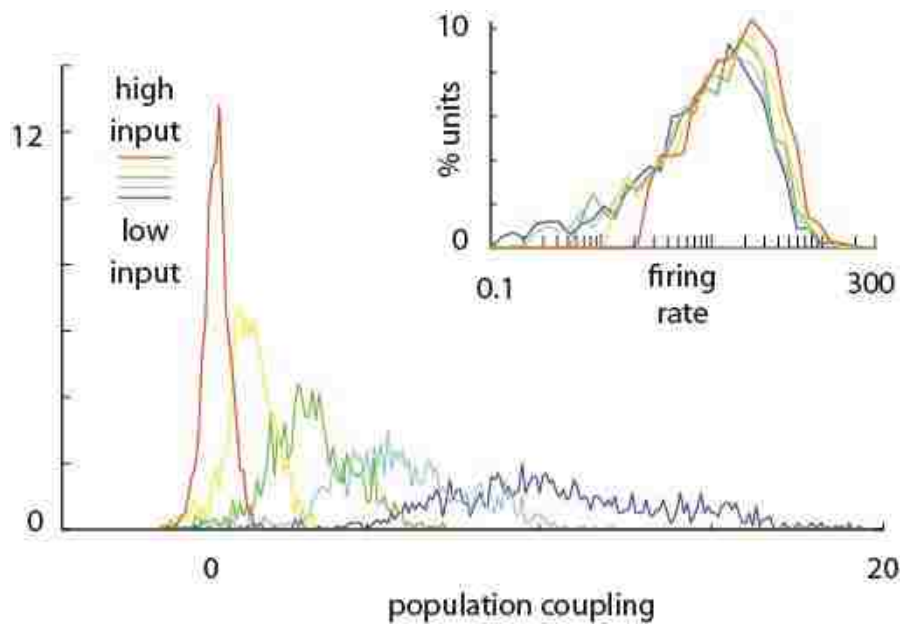
Fig 3) Tuning external input alters the population coupling. Population coupling decreases as external input increases while firing rate(inset) remains constant (strength of inhibition is constant).
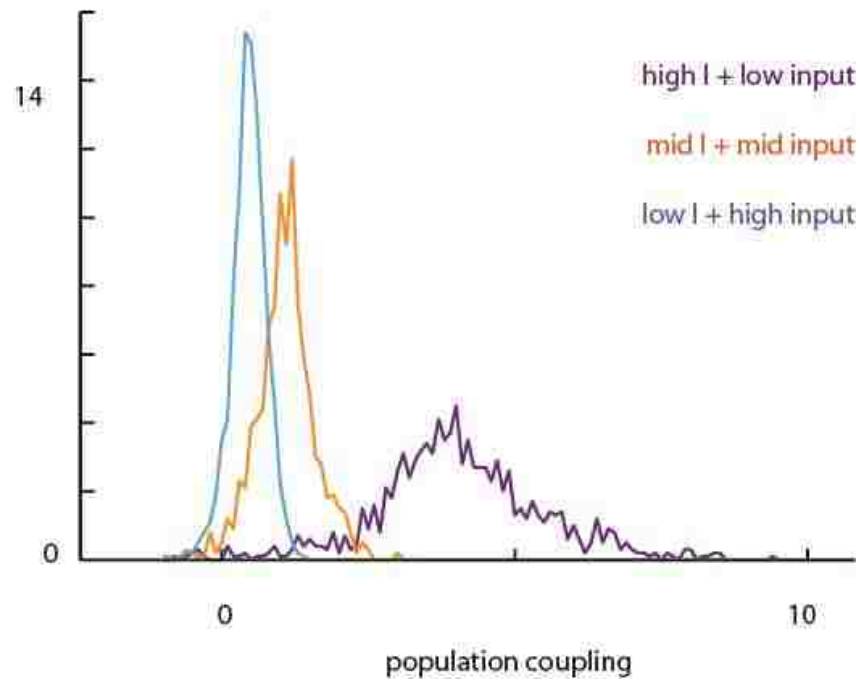

Fig 4) Change of inhibition and external input. Enhanced inhibition with reduced external input increases the population coupling(purple) whereas reduced inhibition and enhanced external input decreases the population coupling(cyan) in contrast to fixed inhibition and external input(orange).

Conclusion

In conclusion, we found neurons imbedded in a large scale network can have different population coupling. Neighboring neurons can be highly or weakly correlated to the population. Locally enhancing the inhibition decreased the population coupling while globally enhancing the inhibition (reducing external input and increasing local inhibition) increased the population coupling. Experiments with global manipulation of inhibition from our lab agree with these predictions so far. We are currently doing additional experiments with local manipulation of inhibition to further test the predictions that come from the model presented in this chapter.

References

1.   Shew, W.L., et al., *Information capacity and transmission are maximized in balanced cortical networks with neuronal avalanches.* J Neurosci, 2011. **31**(1): p. 55-63.

2.   Okun, M., et al., *Diverse coupling of neurons to populations in sensory cortex.* Nature, 2015. **521**(7553): p. 511-515.

3.   Tolhurst, D.J., J.A. Movshon, and A.F. Dean, *The statistical reliability of signals in single neurons in cat and monkey visual cortex.* Vision Res, 1983. **23**(8): p. 775-85.

4.   Zagha, E., X. Ge, and D.A. McCormick, *Competing Neural Ensembles in Motor Cortex Gate Goal-Directed Motor Output.* Neuron, 2015. **88**(3): p. 565-77.

Conclusion

Depending on behavioral context, the cerebral cortex can exhibit dramatic changes in the nature of collective, population neural activity. The overall goal of the work presented in this thesis was to better understand how these changes in cortical state manifest in a three specific aspects of cortex dynamics and function. In all three studies, we generated a continuum of cortical states ranging from asynchronous, weakly correlated activity to large-scale synchronous activity by tuning the balance of inhibition and excitation. In all three studies we combined experimental data and data from computational models.

In first study (chapter I of this thesis), we measured how well the ongoing cortical population activity can be predicted based on its own recent history. The study was performed in anesthetized rat somatosensory cortex and in a computational model. For long time scales (~1 sec), we found that predictability improves as cortical states shifts from synchronized to desynchronized states. For short time period of prediction (~10-100 ms) this trend reverses f in both experiment and computational model. Thus, we can conclude that the intrinsic predictability of cortex network dynamics depends strongly on changes in cortical state.

In another study we compared controllability of network dynamics across the continuum of cortical states using an optogenetic closed-loop feedback system. The study was performed in isoflurane anesthetized mice, in motor cortex, and in a probabilistic integrate-and-fire model of neurons. We observed a strong anti-correlation between the accuracy of the control and the cost of control. The same results were found in the computational model. One interesting implication of these results was that, if the cortex needs to balance between cost and accuracy of control, then it would need

to operate in a cortical state that is not too synchronized and not too desynchronized. The optimal state may lie near the tipping point between these two regimes.

Finally, in a purely computational study, we studied how the activity of single neurons is related to collective spiking activity of a large population in which the single neuron is embedded. More specifically, we studied how the 'population coupling' of individual neurons changes when we tuned the balance of excitation and inhibition of the network. We found that increased inhibition in the brain can have two opposite effects on population coupling. Enhancing the local inhibition decreased population coupling while globally enhancing inhibition might increase population coupling.

Future work

For the feedback control study, the next steps are performing more experiment and collecting more data, and deeper data analysis to assess the cortical states, in order to compare the controllability versus cortical state instead of anesthetic level.

For the population coupling study, experimental tests comparing local versus global manipulation of inhibition are currently underway and we hope to have results on this soon. Depending on the results of these experiments, we may or may not need to improve our model to explain the experimental results.

Appendix

UNIVERSITY OF ARKANSAS

Office of Research Compliance

MEMORANDUM

TO: Dr. Woodrow Shew

FROM: Craig N. Coon, Chairman
           Institutional Animal Care and Use Committee

DATE: June 6, 2014

SUBJECT: IACUC APPROVAL
           Expiration date: June 30, 2017

The Institutional Animal Care and Use Committee (IACUC) has APPROVED your protocol 14048: "Neural correlates of unconstrained behavior in rat models of autism". Your start date is July 1, 2014

In granting its approval, the IACUC has approved only the information provided. Should there be any further changes to the protocol during the research, please notify the IACUC in writing (via the Modification form) prior to initiating the changes. If the study period is expected to extend beyond June 30, 2017 you must submit a new protocol. By policy the IACUC cannot approve a study for more than 3 years at a time.

The IACUC appreciates your cooperation in complying with University and Federal guidelines involving animal subjects.

CNC/aem

cc: Animal Welfare Veterinarian

MEMORANDUM

To: Woodrow Shew
From: Craig Coon, IACUC Chair
Date: August 22, 2016
Subject: IACUC Approval
Expiration Date: August 17, 2019

The Institutional Animal Care and Use Committee (IACUC) has APPROVED your protocol #17003 "Optogenetic dissection of retronasal olfaction" contingent upon your compliance with any stipulations for the use of urethane set forth by the UARK office of Environmental Health and Safety.

In granting its approval, the IACUC has approved only the information provided. Should there be any further changes to the protocol during the research, please notify the IACUC in writing (via the Modification form) prior to initiating the changes. If the study period is expected to extend beyond August 17, 2019 you must submit a newly drafted protocol prior to that date to avoid any interruption. By policy the IACUC cannot approve a study for more than 3 years at a time.

The IACUC appreciates your cooperation in complying with University and Federal guidelines involving animal subjects.

CNC/aem
cc: Animal Welfare Veterinarian

UNIVERSITY OF ARKANSAS.

MEMORANDUM

TO: Woodrow Shew

FROM: Craig N. Coon, Chairman
          Institutional Animal Care
          And Use Committee

DATE: February 8, 2012

SUBJECT: IACUC PROTOCOL **APPROVAL**
            Expiration date : **February 06, 2015**

The Institutional Animal Care and Use Committee (IACUC) has **APPROVED** Protocol **#12025-
"OPTIMIZATION OF SENSORY PROCESSING IN THE RAT WHISKER SYSTEM**". You may
begin this study immediately.

The IACUC encourages you to make sure that you are also in compliance with other UAF committees
such as Biosafety, Toxic Substances and/or Radiation Safety if your project has components that fall
under their purview.

In granting its approval, the IACUC has approved only the protocol provided. Should there be any
changes in the protocol during the research, please notify the IACUC in writing [Modification Request
form] **prior** to initiating the changes. If the study period is expected to extend beyond **02-06-2015,** you
must submit a new protocol. By policy the IACUC cannot approve a study for more than 3 years at a time.

The IACUC appreciates your cooperation in complying with University and Federal guidelines for
research involving animal subjects.

cnc/car

cc: Animal Welfare Veterinarian